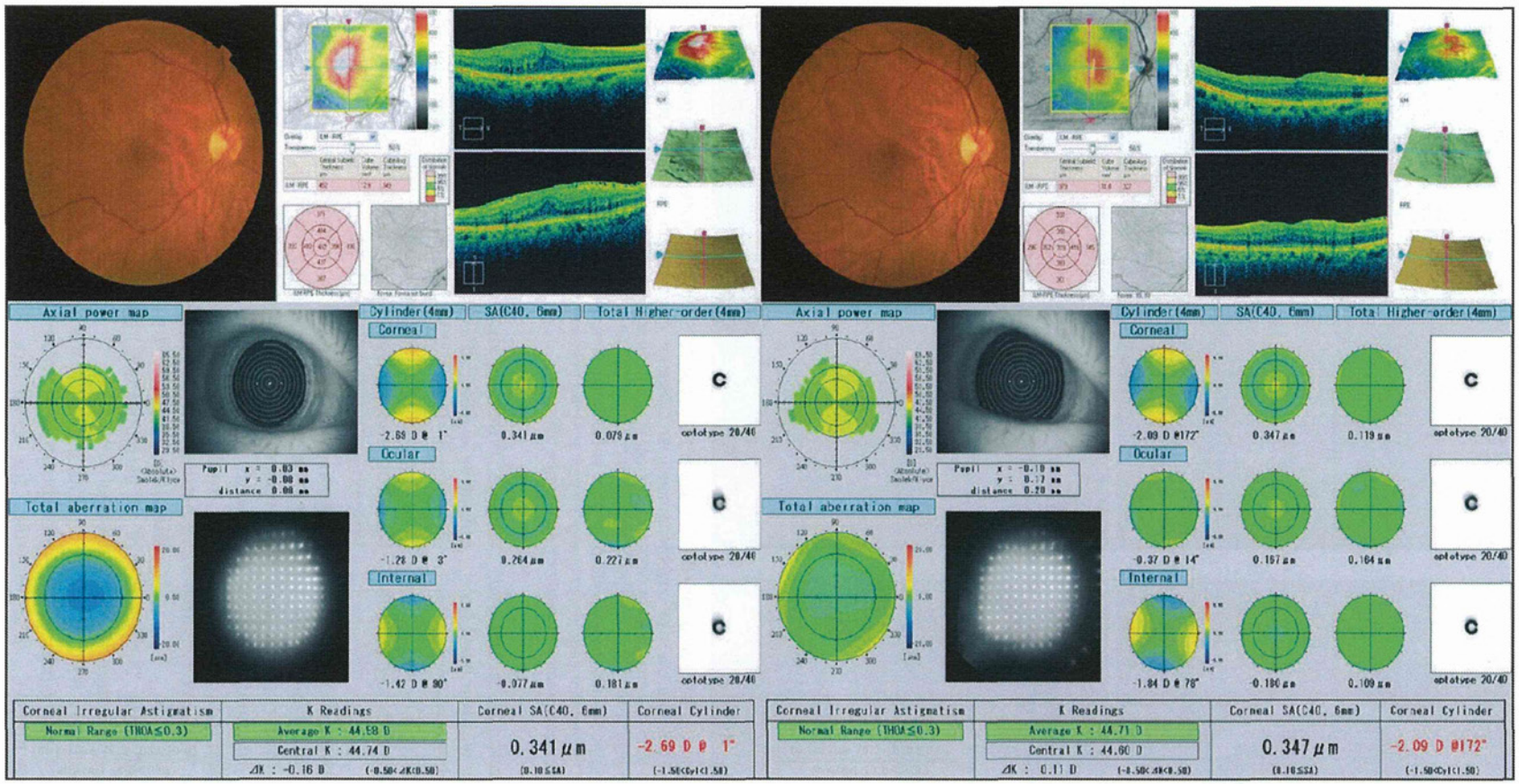

Figure 2. Representative eye (Patient 2 in Table 1) with an epiretinal membrane (ERM) (Patient 2; see Table 1). Preoperative and postoperative findings of the eye of a 60-year-old woman with an ERM. The eye had undergone combined 25-gauge micro incision vitrectomy surgery (25G MIVS) and toric IOL implantation with posterior capsulotomy. (Upper left) Preoperative photograph of the right fundus and findings of optical coherent tomography showing ERM and thickened foveal thickness, respectively. (Upper right) Postoperative photograph of the right fundus and findings of optical coherent tomography showing no ERM and decreased foveal thickness, respectively. (Lower left) Preoperative findings of a wavefront analyzer showing cylindrical with-the-rule corneal astigmatism. The ocular total cylindrical astigmatism was decreased slightly because the internal cylindrical astigmatism (cataract) corrected the corneal astigmatism slightly. Preoperatively, logMAR uncorrected visual acuity (UCVA) and best corrected visual acuity (BCVA) in this eye were 1.15 and 0.05, respectively. (Lower right) Postoperative findings of a wavefront analyzer showing cylindrical with-the-rule corneal astigmatism, unchanged from the preoperative condition. The ocular total cylindrical astigmatism was almost completely corrected postoperatively because the internal cylindrical astigmatism (toric IOL) had a strong corrective effect on the corneal astigmatism. Postoperatively, logMAR UCVA and BCVA in this eye were 0 and –0.08, respectively.

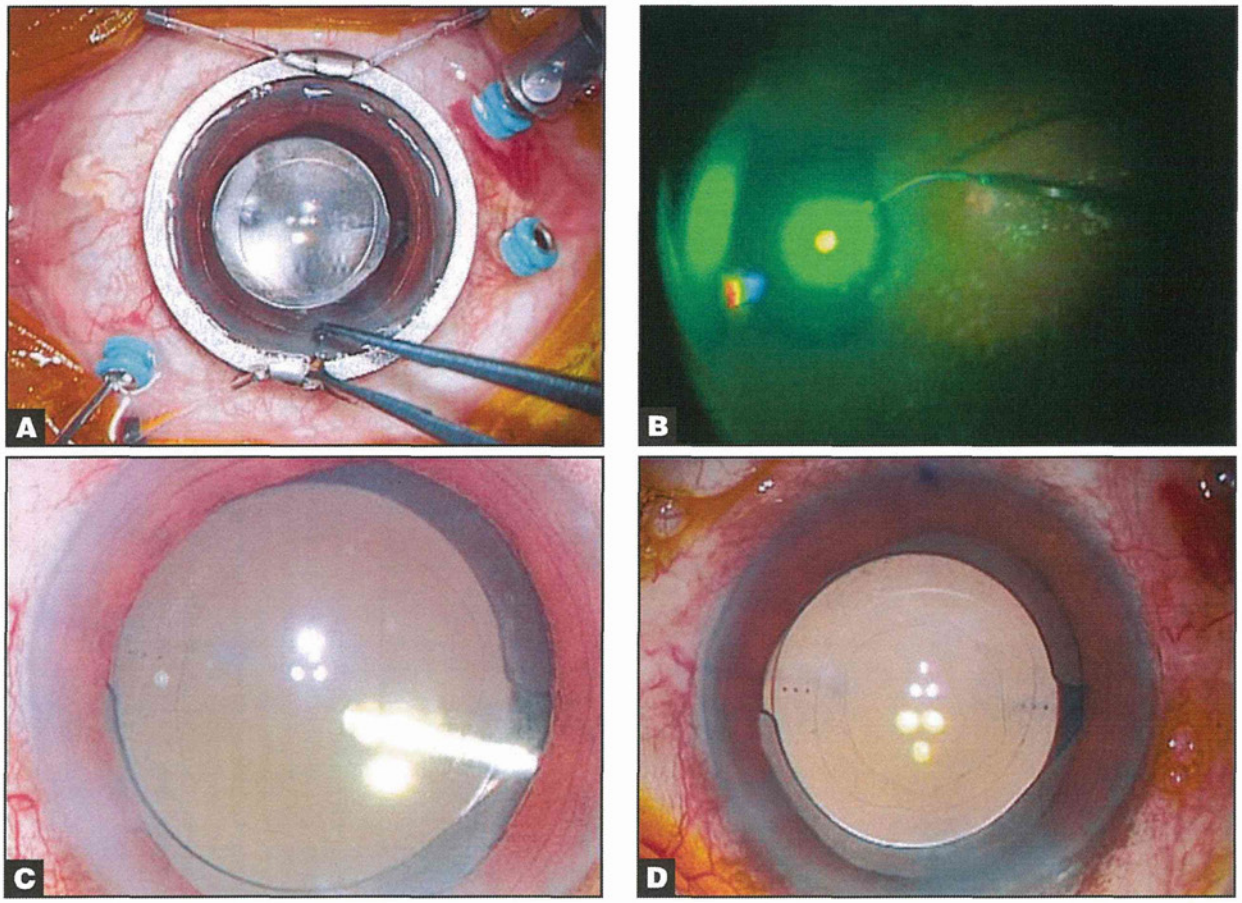

Figure 3. Representative eye with proliferative diabetic retinopathy (PDR) (Patient 12 in Table 1). Fundus and intraoperative photographs of the eye of a 66-year-old woman with PDR. The eye had undergone combined 25-gauge microincision vitrectomy surgery (25G MIVS) using the wide-viewing system and toric IOL implantation with posterior capsulotomy (posterior capsulotomy). (A) Intraoperative photograph of the anterior segment indicating a toric IOL implanted before 25G MIVS. (B) Intraoperative photograph of the fundus showing endolaser photocoagulation being performed to complete panretinal photocoagulation, which was clearly visible thorough a toric IOL. (C) Intraoperative photograph of the anterior segment showing the center of the posterior capsule removed using a 25-gauge vitreous cutter. (D) The posterior capsule has been removed circularly and completely.

and the MH was closed postoperatively. In the eye with PDR, the vitreous hemorrhage was removed successfully and endolaser performed complete panretinal photocoagulation. In all cases, the IOL was stably fixed and remained well-positioned at final examination.

The preoperative absolute corneal cylinder (mean cylinder) was 1.88 ± 0.46 D, and the 1-month postoperative absolute residual refractive cylinder was 0.79 ± 0.53 D. The postoperative residual refractive cylinder was significantly lower than the pre-existing regular corneal cylinder (P = .003, Wilcoxon signed-rank test).

UCVA and BCVA improved in all cases. The mean postoperative logMAR UCVA at 1 and 6 months was 0.31 ± 0.42 and 0.29 ± 0.43, respectively (P = 0.002, Wilcoxon signed-rank test), which was significantly better than the preoperative UCVA of 1.03 ± 0.38 (P = 0.002, Wilcoxon signed-rank test). The mean postoperative logMAR BCVA at 1 and 6 months was 0.05 ± 0.18 and −0.02 ± 0.13 (P = .023, Wilcoxon signed-rank test), respectively, which was significantly better than the preoperative BCVA of 0.34 ± 0.38 (P = .015, Wilcoxon signed-rank test). There was no difference between logMAR UCVA at 1 and 6 months (P = .69, Wilcoxon signed-rank test) or logMAR BCVA at 1 and 6 months (P = .35, Wilcoxon signed-rank test). The logMAR UCVA and BCVA improved to zero or less at 1 month in three of 12 patients (25%) and seven of 12 patients (58%), respectively. The logMAR UCVA and BCVA improved to 0 or less at 6 months in four of 12 patients (33%) and nine of 12 patients (75%), respectively.

In all cases, the IOL was stably fixed and remained well-positioned without a remarkable degree of rotation. The mean toric IOL axis rotation at 1 week, 1

month, and 6 months postoperatively was 5.8 ± 4.1°, 6.4 ± 4.0°, and 5.7 ± 3.1°, respectively, and the values were statistically similar at 1 week, 1 month, and 6 months (P = .64, Friedman test).

We did not suture the corneal wound or scleral ports in any of our cases. There were no intraoperative complications. In the eye with PDR, there was a temporary postoperative posterior iris synechia, but it released naturally, without any additional surgical intervention. No PCO, bacterial endophthalmitis, or other postoperative complications occurred.

Intraoperative findings in a representative case with ERM (Patient 2 in Table 1) are shown in Figure 1. Preoperative and postoperative findings in the same case (Patient 2 in Table 1) are shown in Figure 2. Intraoperative findings in a representative case with PDR (Patient 12 in Table 1) are shown in Figure 3. Preoperative and postoperative findings in the same case (Patient 12 in Table 1) are shown in Figure 4.

DISCUSSION

We set out to evaluate the efficacy of combined 25G MIVS and toric IOL implantation with posterior capsulotomy. Our study shows that this procedure is a practical and safe method for use in eyes with both vitreoretinal disease and corneal astigmatism. We observed a postoperative residual refractive cylinder significantly lower than the pre-existing regular corneal cylinder, as well as very rapid and sustained improvement of postoperative vision, with no occurrence of PCO. Axis rotation of the toric IOLs was minimal, and they were stably fixed 1 week postoperatively, and remained thus 6 months postoperatively.

Our study supports existing evidence that rapid visual improvement time makes 25G MIVS preferable to conventional 20-gauge pars plana vitrectomy (PPV) for the treatment of macular pucker or macular hole.[3,6] When 20-gauge PPV is used, suturing of the sclerotomy sites is required, and the sutures can induce postoperative astigmatism.[2,3,5-7] Our study also confirms existing data showing that acrylic toric IOLs are rotationally stable in the first 6 months postoperatively.[29,30] Furthermore, our study confirms existing data showing that 25G MIVS with posterior capsulotomy can prevent PCO.[26,27]

To achieve high-quality vision at an early postoperative stage in patients with retinal disease and corneal astigmatism, it is necessary to both correct the corneal astigmatism and thoroughly treat the retinal disease. The astigmatism of cataracts can offset corneal astigmatism (Figure 2), which then affects vision negatively after 25G MIVS and conventional (nontoric) IOL implantation. Currently, many patients over 50 years of age with retinal disease and cataract undergo a combination of 25G MIVS and IOL implantation, because if the cataract is left, it will progress after the operation. However, many such patients have regular corneal astigmatism and would benefit from use of a toric rather than conventional IOL. We believe that eyes with ERM, in particular, that start with high visual acuity should undergo combined 25G MIVS and toric IOL implantation if the eyes meet the criteria.

In our procedures, we simultaneously performed posterior capsulotomy. In posterior capsulotomy, the loss of the barrier between the anterior chamber and vitreous cavity raises concern about the possibility of postoperative endophthalmitis, but none occurred in our cases. We have reported that gas leaked from the vitreous cavity, through the posterior capsulotomy, and into the anterior chamber in cases in which fluid-air exchange was performed.[27] Thus, there was concern about the possibility of postoperative rotation of the toric IOL in our three cases with MH, because gas tamponade and a prone position can have negative effects on the implanted toric IOL. However, we saw no remarkable degree of rotation.

There are two advantages to combining 25G MIVS and toric IOL implantation with posterior capsulotomy. First, in patients with vitreoretinal disease requiring a vitrectomy combined with cataract surgery, a primary posterior capsulotomy technique using a 25-gauge vitreous cutter can prevent postoperative posterior capsule opacification,[26] thereby avoiding additional Nd:YAG laser treatment.[27] Secondly, posterior capsulotomy can release the fluid between the IOL and posterior capsule into the vitreous cavity, so that the posterior capsule can completely attach to the posterior surface of the IOL. This may prevent intraoperative and postoperative IOL rotation. Although fluid/air exchange was performed after the insertion of a toric IOL in cases with MH, the toric IOL was sufficiently stable, and there was no remarkable degree of axis rotation intraoperatively or postoperatively (Table 1, Patients 9 through 11). In our cases, the mean toric IOL axis rotation was statistically similar 1 week, 1 month, and 6 months postoperatively, and the mean rotation at 6 months was within 6°.

We did not have any visual difficulties in peeling ERMs and ILMs when the 25-gauge instruments were seen through the implanted toric IOL (Figure 1, upper right). We believe that during macular surgery for toric IOL-implanted eyes, vitreous surgeons should not experience any problems visualizing the macular lesion, because toric IOLs are made for the macula to focus on with less astigmatism. By contrast, if a peripheral lesion were seen through a floating contact lens and peripheral toric IOL, there could be prob-

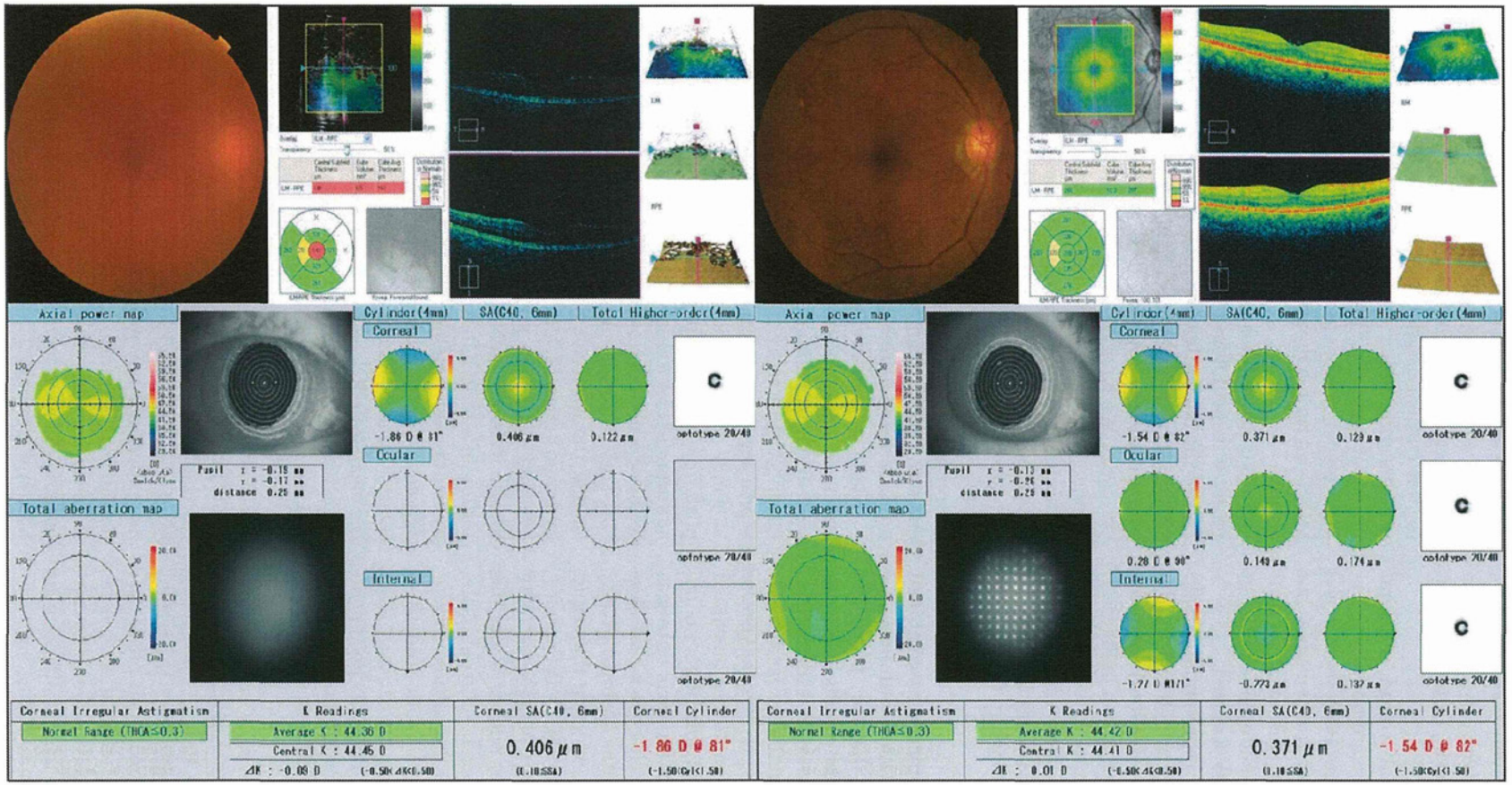

Figure 4. Representative eye (Patient 12 in Table 1) with proliferative diabetic retinopathy (PDR) (Patient 12; see Table 1). Preoperative and postoperative findings of the eye of a 66-year-old woman with PDR. The eye had undergone combined 25-gauge microincision vitrectomy surgery (25G MIVS) and toric IOL implantation with posterior capsulotomy. (Upper left) Preoperative photograph of the right fundus and findings of optical coherent tomography showing vitreous hemorrhage (VH) and low signal intensity due to VH, respectively. (Upper right) Postoperative photograph of the right fundus and findings of optical coherent tomography showing no VH and good foveal centralis, respectively. (Lower left) Preoperative findings of a wavefront analyzer showing cylindrical against-the-rule corneal astigmatism. The internal and ocular total astigmatism could not be detected due to VH. Preoperatively, logMAR uncorrected visual acuity (UCVA) and best corrected visual acuity (BCVA) in this eye were 1.40 and 1.15, respectively. (Lower right) Postoperative findings of a wave-front analyzer showing cylindrical against-the-rule corneal astigmatism, unchanged from the preoperative condition. Internal and ocular total astigmatism could be detected because VH had been successfully removed by the 25G MIVS procedure. The ocular total cylindrical astigmatism was almost completely corrected postoperatively because the internal cylindrical astigmatism (toric IOL) had a strong corrective effect on the corneal astigmatism. Postoperatively, logMaAR UCVA and BCVA in this eye were both –0.08.

lems visualizing the peripheral lesion. However, the wide-viewing system should eliminate any trouble visualizing the macular and peripheral regions, because the system can theoretically visualize all retinal lesions solely through the small central region of the toric IOL. This region has little corrective effect on astigmatism, and the possibility of visual distortion for the surgeon is thus minimal. In fact, we used the wide-viewing system to perform peripheral vitrectomy and panretinal endolaser photocoagulation for the PDR eye (Patient 12 in Table 1; Figure 1, upper right) without difficulty. Thus, we recommend that a toric IOL should be inserted in the first half of the combined surgery (before vitrectomy), following which 25G MIVS should be performed through a conventional contact lens for the macular region and through the wide-viewing system for the peripheral region.

The reason why the toric IOL should be inserted in the first half of the combined surgery is to confirm its rotational stability. If the toric IOL were inserted at the end of the vitrectomy, the rotational stability of the toric IOL could not be completely confirmed intraoperatively. Vitreous surgeons need to confirm the stability of the toric IOL intraoperatively because of the chance that the implanted toric IOL could be unstable at an early phase after its insertion. However, we believe that in our cases, the toric IOL with posterior capsulotomy was stably positioned several minutes after insertion. We have previously reported the difficulty of seeing through the implanted IOL with posterior capsulotomy in cases in which fluid-air exchange is used.[27] This is because the retro-surface of the IOL can have an irregular reflex, or there can be dew in the fluid-air exchange. Therefore, in cases with retinal detachment that are expected to require intraoperative fluid-air exchange, phacovitrectomy with a toric IOL and posterior capsulotomy should be performed with caution.

If postoperative iris synechiae occur, the implanted toric IOL can be affected and become tilted. Therefore, it might be advisable to avoid our procedure in cases such as severe PDR, proliferative vitreoretinopathy (PVR), or uveitis, because they require lengthy surgery to treat the proliferative tissue and an injection of perfluoropropane.[31] However, we believe that under favorable conditions in the anterior and posterior segments, our technique is the best approach to treating retinal diseases with corneal astigmatism to achieve the highest quality of postoperative vision. Thus, preoperative examination of lenticular and retinal conditions is very important when considering 25G MIVS and toric IOL implantation with posterior capsulotomy.

The limitations of our study include its retrospective nature, small patient population, and short follow-up period. In addition, retinal diseases with corneal astigmatism can be accompanied by severe PDR, PVR, weak zonules, or pseudoexfoliation syndrome. Retinal conditions such as longstanding macula-off PDR or PVR would not be suitable for implanting a toric IOL using this technique, because the postoperative visual prognosis would be poor. Anterior conditions such as weak zonules or pseudoexfoliation syndrome would also contraindicate implanting a toric IOL using this technique because of the postoperative instability of the capsular bag.

In conclusion, it is possible to fix a toric IOL with posterior capsulotomy during 25G MIVS. This procedure is a practical and safe approach in eyes with concurrent vitreoretinal disease and corneal astigmatism. The pre-existing regular corneal cylinder is corrected efficiently and stably, and the improvement in postoperative vision is rapid and sustained, with no occurrence of PCO. Further investigation toward establishing this procedure as standard is merited. Taking corneal astigmatism into consideration when patients with retinal disease require surgical intervention may result in higher postoperative visual function.

REFERENCES

1. Galway G, Drury B, Cronin BG, Bourke RD. A comparison of induced astigmatism in 20- vs 25-gauge vitrectomy procedures. *Eye (Lond).* 2010;24(2):315-317.
2. Avitabile T, Castiglione F, Bonfiglio V. Transconjunctival sutureless 25-gauge versus 20-gauge standard vitrectomy: correlation between corneal topography and ultrasound biomicroscopy measurements of sclerotomy sites. *Cornea.* 2010;29(1):19-25.
3. Shinoda H, Shinoda K, Satofuka S, et al. Visual recovery after vitrectomy for macular hole using 25-gauge instruments. *Acta Ophthalmol.* 2008;86(2):151-155.
4. Valmaggia C. Pars plana vitrectomy with 25-gauge instruments in the treatment of idiopathic epiretinal membranes. *Klin Monbl Augenheilkd.* 2007;224(4):292-296.
5. Okamoto F, Okamoto C, Sakata N, et al. Changes in corneal topography after 25-gauge transconjunctival sutureless vitrectomy versus after 20-gauge standard vitrectomy. *Ophthalmology.* 2007;114(12):2138-2141.
6. Kadonosono K, Yamakawa T, Uchio E, et al. Comparison of visual function after epiretinal membrane removal by 20-gauge and 25-gauge vitrectomy. *Am J Ophthalmol.* 2006;142(3):513-515.
7. Yanyali A, Celik E, Horozoglu F, Nohutcu AF. Corneal topographic changes after transconjunctival (25-gauge) sutureless vitrectomy. *Am J Ophthalmol.* 2005;140(5):939-941.
8. Mendicute J, Irigoyen C, Aramberri J, Ondarra A, Montés-Micó R. Foldable toric intraocular lens for astigmatism correction in cataract patients. *J Cataract Refract Surg.* 2008;34(4):601-607.
9. Till JS, Yoder PR Jr., Wilcox TK, Spielman JL. Toric intraocular lens implantation: 100 consecutive cases. *J Cataract Refract Surg.* 2002;28(2):295-301.
10. Ruhswurm I, Scholz U, Zehetmayer M, Hanselmayer G, Vass C, Skorpik C. Astigmatism correction with a foldable toric intraocular lens in cataract patients. *J Cataract Refract Surg.* 2000;26(7):1022-1027.
11. Ferrer-Blasco T, Montés-Micó R, Peixoto-de-Matos SC, González-

Méijome JM, Cerviño A. Prevalence of corneal astigmatism before cataract surgery. *J Cataract Refract Surg.* 2009;35(1):70-75.
12. Fujii GY, De Juan E, Jr., Humayun MS, et al. A new 25-gauge instrument system for transconjunctival sutureless vitrectomy surgery. *Ophthalmology.* 2002;109(10):1807-1812.
13. Fujii GY, De Juan E, Jr., Humayun MS, et al. Initial experience using the transconjunctival sutureless vitrectomy system for vitreoretinal surgery. *Ophthalmology.* 2002;109(10):1814-1820.
14. Kunikata H, Nitta F, Meguro Y, et al. Difficulty in inserting 25- and 23-gauge trocar cannula during vitrectomy. *Ophthalmologica.* 2011;226(4):198-204.
15. Shimada H, Nakashizuka H, Mori R, Mizutani Y. Expanded indications for 25-gauge transconjunctival vitrectomy. *Jpn J Ophthalmol.* 2005;49(5):397-401.
16. Gonzales CR, Boshra J, Schwartz SD. 25-Gauge pars plicata vitrectomy for stage 4 and 5 retinopathy of prematurity. *Retina.* 2006;26(7 Suppl):S42-6.
17. Riemann CD, Miller DM, Foster RE, Petersen MR. Outcomes of transconjunctival sutureless 25-gauge vitrectomy with silicone oil infusion. *Retina.* 2007;27(3):296-303.
18. Kadonosono K, Yamakawa T, Uchio E, et al. Fibrovascular membrane removal using a high-performance 25-gauge vitreous cutter. *Retina.* 2008;28(10):1533-1535.
19. Kiss S, Vavvas D. 25-gauge transconjunctival sutureless pars plana vitrectomy for the removal of retained lens fragments and intraocular foreign bodies. *Retina.* 2008;28(9):1346-1351.
20. Lai MM, Ruby AJ, Sarrafizadeh R, et al. Repair of primary rhegmatogenous retinal detachment using 25-gauge transconjunctival sutureless vitrectomy. *Retina.* 2008;28(5):729-734.
21. Kunikata H, Nishida K. Visual outcome and complications of 25-gauge vitrectomy for rhegmatogenous retinal detachment; 84 consecutive cases. *Eye (Lond).* 2010;24(6):1071-1077.
22. Farouk MM, Naito T, Sayed KM, et al. Outcomes of 25-gauge vitrectomy for proliferative diabetic retinopathy. *Graefes Arch Clin Exp Ophthalmol.* 2011;249(3):369-376.
23. Kunikata H, Abe T, Nishida K. Successful outcomes of 25- and 23-gauge vitrectomies for giant retinal tear detachments. *Ophthalmic Surg Lasers Imaging.* 2011;42(6):487-492.
24. Kunikata H, Fuse N, Abe T. Fixating dislocated intraocular lens by 25-gauge vitrectomy. *Ophthalmic Surg Lasers Imaging.* 2011;42(4):297-301.
25. Kunikata H, Uematsu M, Nakazawa T, Fuse N. Successful removal of large intraocular foreign body by 25-gauge microincision vitrectomy surgery. *J Ophthalmol.* 2011;2011:940323.
26. Sato S, Inoue M, Kobayashi S, Watanabe Y, Kadonosono K. Primary posterior capsulotomy using a 25-gauge vitreous cutter in vitrectomy combined with cataract surgery. *J Cataract Refract Surg.* 2010;36(1):2-5.
27. Aizawa N, Kunikata H, Abe T, Nakazawa T. Efficacy of combined 25-gauge microincision vitrectomy, intraocular lens implantation, and posterior capsulotomy. *J Cataract Refract Surg.* 2012;38(9):1602-1607.
28. Shimada H, Nakashizuka H, Mori R, Mizutani Y, Hattori T. 25-gauge scleral tunnel transconjunctival vitrectomy. *Am J Ophthalmol.* 2006;142(5):871-873.
29. Mingo-Botín D, Muñoz-Negrete FJ, Won Kim HR, Morcillo-Laiz R, Rebolleda G, Oblanca N. Comparison of toric intraocular lenses and peripheral corneal relaxing incisions to treat astigmatism during cataract surgery. *J Cataract Refract Surg.* 2010;36(10):1700-1708.
30. Koshy JJ, Nishi Y, Hirnschall N, et al. Rotational stability of a single-piece toric acrylic intraocular lens. *J Cataract Refract Surg.* 2010;36(10):1665-1670.
31. Kim SW, Oh J, Song JS, Kim YY, Oh IK, Huh K. Risk factors of iris posterior synechia formation after phacovitrectomy with three-piece acrylic IOL or single-piece acrylic IOL. *Ophthalmologica.* 2009;223(4):222-227.

Journal of Neurochemistry

JOURNAL OF NEUROCHEMISTRY | 2013 | 125 | 713–723

doi: 10.1111/jnc.12132

ORIGINAL ARTICLE

Novel neuroprotective action of prothymosin alpha-derived peptide against retinal and brain ischemic damages

Sebok Kumar Halder, Hayato Matsunaga, Haruka Yamaguchi and Hiroshi Ueda

Department of Molecular Pharmacology and Neuroscience, Nagasaki University Graduate School of Biomedical Sciences, Nagasaki, Japan

Abstract

Prothymosin alpha (ProTα), a nuclear protein, is implicated in the inhibition of ischemia-induced necrosis as well as apoptosis in the brain and retina. Although ProTα has multiple biological functions through distinct regions in its sequence, it has remained which region is involved in this neuroprotection. This study reported that the active core peptide sequence P_{30} (amino acids 49–78) of ProTα exerts its full survival effect in cultured cortical neurons against ischemic stress. Our *in vivo* study revealed that intravitreous administration of P_{30} at 24 h after retinal ischemia significantly blocks the ischemia-induced functional damages of retina at day 7. In addition, P_{30} completely rescued the retinal ischemia-induced ganglion cell damages at day 7 after the ischemic stress, along with partial blockade of the loss of bipolar, amacrine, and photoreceptor cells. On the other hand, intracerebroventricular (3 nmol) or systemic (1 mg/kg; i.v.) injection of P_{30} at 1 h after cerebral ischemia (1 h tMCAO) significantly blocked the ischemia-induced brain damages and disruption of blood vessels. Systemic P_{30} delivery (1 mg/kg; i.v.) also significantly ameliorated the ischemic brain caused by photochemically induced thrombosis. Taken together, this study confers a precise demonstration about the novel protective activity of ProTα-derived small peptide P_{30} against the ischemic damages *in vitro* and *in vivo*.

Keywords: blood vessel, brain ischemia, neuroprotective peptide, prothymosin alpha, retinal ischemia.

J. Neurochem. (2013) **125**, 713–723.

Ischemic damages in the central nervous system including brain and retina are associated with the rapid and severe loss of functional and cellular responses through the mechanisms of necrosis as well as apoptosis by several types of cytotoxic mediators (White *et al.* 2000; Paolucci *et al.* 2003; Ueda and Fujita 2004; Feigin 2005; Flynn *et al.* 2008; Fornage 2009; Dvoriantchikova *et al.* 2010; Neroev *et al.* 2010; Sims and Muyderman 2010; Yin *et al.* 2010; Iadecola and Anrather 2011; Witmer *et al.* 2011). At the same time, several neuroprotective molecules such as brain-derived neurotrophic factor (BDNF), fibroblast growth factor (FGF), and erythropoietin (EPO) are produced upon ischemia to play limited attenuation of ischemic damages through the anti-apoptosis mechanisms, without exerting protective activity against necrosis (Siren *et al.* 2001; Korada *et al.* 2002; Maiese *et al.* 2004; Blanco *et al.* 2008; Fujita *et al.* 2009; Madinier *et al.* 2009; Ueda *et al.* 2010; Bejot *et al.* 2011).

Prothymosin alpha (ProTα) has been identified in the conditioned medium of serum-free primary culture of cortical neurons, as an anti-necrosis factor (Ueda *et al.* 2007). In addition, ProTα potently inhibits the ischemia-induced damages in brain and retina (Fujita and Ueda 2007; Fujita *et al.* 2009; Ueda *et al.* 2010). It is interesting that ProTα

Received October 25, 2012; revised manuscript received December 3, 2012; accepted December 4, 2012.

Address correspondence and reprint requests to Dr. Hiroshi Ueda, Department of Molecular Pharmacology and Neuroscience, Nagasaki University Graduate School of Biomedical Sciences, 1-14 Bunkyo-machi, Nagasaki 852-8521, Japan.

E-mail: ueda@nagasaki-u.ac.jp

Abbreviations used: a.a., amino acid; BDNF, brain-derived neurotrophic factor; Chx10, ceh-10 homeodomain-containing homolog; ERG, electroretinogram; GCL, ganglion cell layer; H&E, hematoxylin and eosin; i.c.v., intracerebroventricularly; i.v., intravenously; i.vt., intravitreously; INL, inner nuclear layer; IPL, inner plexiform layer; NeuN, neuronal nuclei; ONL, outer nuclear layer; P_{30}, peptide sequence comprised of 30 amino acids; PIT, photochemically induced thrombosis; ProTα, prothymosin alpha; tMCAO, transient middle cerebral artery occlusion; TTC, 2,3,5–triphenyltetrazolium chloride.

has distinct actions, which are all related to the cell survival (Jiang *et al.* 2003; Ueda 2008; Mosoian *et al.* 2010; Ueda *et al.* 2012). Some studies revealed that different peptide sequences in ProTα are implicated with these survival actions. The peptide sequence in the central domain of ProTα (amino acids; a.a. 32–52) is related to the interaction with Kelch-like ECH-associated protein 1 (Keap1), which play roles in the induction of oxidative stress-protecting genes expression by liberating Nrf2 from the Nrf2-Keap1 inhibitory complex (Karapetian *et al.* 2005). The N-terminal sequence in ProTα (a.a. 2–29), corresponding to thymosin alpha 1, which has an ability to induce anti-cancer effects (Garaci *et al.* 2007; Danielli *et al.* 2012). In addition, thymosin alpha 1 has been approved in 35 countries for the treatment of hepatitis B and C, and as an immune stimulant and adjuvant (Goldstein and Goldstein 2009; Pierluigi *et al.* 2010). Previous reports suggested that C-terminal region (a.a. 89–109, 99–109 and 100–109) of human ProTα exerts immunoenhancing effects including pro-inflammatory activity through the stimulation of monocytes via toll-like receptor (TLR) signaling, induces dendritic cell maturation and adopts β-sheet conformation (Skopeliti *et al.* 2009). Most recently, there is a report about the survival activity of the middle part (a.a. 41–83) of human ProTα against mutant huntington-caused cytotoxicity in the cultured cells (Dong *et al.* 2012). However, it remains to be elucidated which region is responsible for the neuroprotection against ischemia-induced neuronal damages. In this study, we have attempted to see the neuroprotective activity of ProTα-derived small peptide against ischemic damages *in vitro* and *in vivo*.

Materials and methods

Animals

Male C57/BLJ mice weighing 20–25 g were purchased from Tagawa Experimental Animals (Nagasaki, Japan) and used for all the experiments. Mice were kept in a room maintained at constant temperature (21 ± 2°C) and relative humidity (55 ± 5%) with an automatic 12 h light/dark cycle with free access to standard laboratory diet and tap water. Animal care and all experimental procedures were formally approved by Nagasaki University Animal Care and Use Committee (Animal Experiments Approval Number: 1104190914).

Expression constructs and purification procedures for GST-fusion rat ProTα deletion mutants

The rat ProTα gene was amplified from cDNA derived from rat embryonic brain. The gene constructions for expression of recombinant GST-ProTα deletion mutants (Full-length, Δ1-29, Δ1-48, Δ1-68, Δ1-86, Δ30-112, Δ58-112, Δ79-112, and Δ102-112) were previously described (Ueda *et al.* 2007; Matsunaga and Ueda 2010). Here, we newly made a GST-ProTα-49-78. The amplified genes blunted at their 5′-ends and cloned in-frame into the BamHI (blunted)-EcoRI sites of pGEX-5X-1 (GE Healthcare Bio-Science Corp, Piscataway, NJ, USA). The PCR primers used were as follows: Δ1-48-F, 5′-AGGGATCCAATGGCTGACAATGAGGT AGATG-3′ and Δ79-112-R, 5′-TTGAATTCCTAATCTCCATC TTCTTCCTC-3′. F-primer contains a BamHI site, while all R-primer contains a stop codon and an EcoRI site. The recombinant proteins were purified using Glutathione-Sepharose™ (GE Healthcare Bio-Science Corp).

Identification of functional active core domain in ProTα

To determine the active core domain in ProTα, we measured the survival activity in primary cultured rat cortical neurons. The preparation and culture of cortical neurons were previously described (Ueda *et al.* 2007). The culture of neurons was started at low density (1×10^5 cells/cm^2) under the serum-free conditions in the presence or absence of GST and GST-ProTα deletion mutants (100 nM). After 12 h from the start of culture, survival activity was evaluated by WST-8 reduction activity (Cell Counting Kit-8; DOJINDO, Kumamoto, Japan). Finally, we successfully obtained the functional active core domain comprised of 30 amino acids in ProTα (a.a. 49–78) and referred as P_{30} according to number of amino acids.

Peptide administration

Intravitreal injection was performed using a 33-gauge needle connected to a microsyringe and the needle was inserted approximately 1 mm behind the corneal limbus, guided under a stereoscopic microscope to avoid lens and retinal injury. Peptide P_{30} was dissolved in 0.05% dimethyl sulfoxide (DMSO), which was diluted with 0.1 M potassium-free phosphate buffered saline (K^+-free PBS). P_{30} was injected intravitreously (i.vt.) in the eye with doses of 1, 3 and 10 pmol/μL at 24 h after retinal ischemia ($n = 5$, $n = 6$ and $n = 7$, respectively). Vehicle was treated with equal volume of 0.05% DMSO in a similar manner. On the other hand, P_{30} was injected intracerebroventricularly (0.03 and 3 nmol/5 μL, i.c.v.; $n = 6$ and $n = 7$, respectively) in the brain at 1 h after cerebral ischemia (1 h tMCAO). P_{30} (0.3 and 1 mg/kg) was administered intravenously (i.v.) at 1 h after cerebral ischemia. In addition, P_{30} was delivered (1 mg/kg, i.v.) at 3 and 6 h after the cerebral ischemic stress.

Retinal ischemia

Retinal ischemia was performed following the method as described previously (Fujita *et al.* 2009). Briefly, mice were anesthetized with an intraperitoneal (i.p.) injection of sodium pentobarbital (50 mg/kg) and pupils were fully dilated with 1% atropine sulfate drops (Nitten, Nagoya, Japan). The anterior chamber of the eye was cannulated with a 33-gauge needle attached to an infusion container of sterile intraocular irrigating solution (BSS PLUS dilution buffer; Alcon, Fort Worth, TX, USA). Retinal ischemia was induced by elevating the IOP to generate a hydrostatic pressure of 130 mm Hg for 45 min by lifting the container. Following 45 min after retinal ischemic stress, the needle was withdrawn and 0.3% ofloxacin (Santen Pharmaceutical Co. Ltd., Osaka, Japan) was applied topically into the eye to avoid infection.

Electroretinogram

Electroretinogram (ERG) study was performed following the protocol as previously described (Fujita *et al.* 2009). Briefly, mice were dark-adapted for 3–4 h, then anesthetized with intraperitoneal injection of pentobarbital sodium (50 mg/kg) and pupils were

dilated with 1% atropine. A contact electrode (KE–S; Kyoto contact lenses, Kyoto, Japan) was placed topically on the corneal apex and reference electrode was placed near the ipsilateral eye. The ground was a subdermal platinum needle electrode near the abdominal area. ERGs were produced by 20 J flash intensities. The flash stimulus source (SLS-3100; Nihon Kohden, Tokyo, Japan) illuminated the eye by diffuse reflection off the interior surface of the ganzfeld. Maximum flash luminance was measured with detector (MEB–9104; Nihon Kohden). After the intensity series, an incandescent background light sufficient to desensitize the rod system was turned on, and ERGs produced by the standard stimulus were recorded every 2 min for 20 min. The background was then turned off, and ERGs were produced by the standard stimulus every 2 min for the first 30 min of dark adaptation. The a- and b-wave amplitudes were measured online (Neuropack m, QP-903B; Nihon Kohden). ERG was performed at day 7 after retinal ischemia.

Middle cerebral artery occlusion model

The transient middle cerebral artery occlusion (tMCAO) model was induced following the method as described previously (Halder *et al.* 2012). Briefly, mice were anesthetized by 2% isoflurane (Mylan, Tokyo, Japan), and body temperature was monitored and maintained at 37°C during surgery. After a midline neck incision, the middle cerebral artery was occluded transiently using 8-0 in size monofilament nylon surgical suture (Natsume Co. Ltd., Tokyo, Japan) coated with silicon (Xantopren, Bayer dental, Osaka, Japan) that was inserted through the left common carotid artery and advanced into the left internal carotid artery. Following 1 h tMCAO, the animals were briefly re-anesthetized with isoflurane and the monofilament was withdrawn for reperfusion studies. Cerebral blood flow was monitored by laser Doppler flowmeter (ALF21; Advance Co., Tokyo, Japan) using a probe (diameter 0.5 mm) of a laser Doppler flowmeter (ALF2100; Advance Co.) inserted into the left striatum (anterior: −0.5 mm, lateral: 1.8 mm from bregma; depth: 4.2 mm from the skull surface) through a guide cannula.

Photochemically induced middle cerebral artery thrombosis

Photochemically induced thrombosis (PIT) was produced following the protocol as described previously (Nagai *et al.* 2007). Briefly, anesthesia was induced with 3% isoflurane, and the rectal temperature was maintained at 37°C. The temporal muscle was dissected, the skull was exposed, and a 1.5-mm opening was made over the middle cerebral artery (MCA). Photo-illumination of green light (wavelength: 540 nm) was achieved with a xenon lamp (model L-4887, Hamamatsu Photonics, Hamamatsu, Japan) with heat-absorbing and green filters, via an optic fiber with a focus of 1 mm, placed on the opening in the skull. Rose Bengal (Wako, Osaka, Japan) was injected (3 mg/kg, i.v.) in mice, and photo-illumination (5000 lx) was applied for 10 min, after which the temporal muscle and skin were replaced. The MCA occlusion time (from the start of light exposure until the flow in the MCA is stopped) was monitored by observation in real time under the microscope.

Retinal and brain tissue preparation

For retinal tissue preparation, mice were deeply anaesthetized with sodium pentobarbital (50 mg/kg, i.p.). Eye was quickly isolated, washed with saline and 4% paraformaldehyde (PFA). Eye was then nicked through pupil, post-fixed in 4% PFA for 24 h and finally transferred to 25% sucrose solution (in 0.1 M K^+-free PBS) overnight for cryoprotection. Following frozen in cryoembedding compound, retinal sections were prepared at 10 μm thickness. For brain tissue preparation, mice were deeply anesthetized with sodium pentobarbital (50 mg/kg, i.p.) and perfused transcardially with 0.1 M PBS, followed by 4% PFA. Brain was then quickly removed, post-fixed in 4% PFA and transferred immediately to 25% sucrose solution overnight. Brain was frozen in cryoembedding compound and coronal sections were cut at 30 μm thickness for immunohistochemical analysis.

Hematoxylin and eosin staining

For hematoxylin and eosin (H&E) staining, frozen retinal sections were washed with 0.1 M K^+-free PBS, immerged in Mayer's hematoxylin solution (Wako) for 5 min at 25°C and then washed with tap water for 20 min. Following brief treatment with 95% ethanol, sections were immerged in eosin-alcohol solution (Wako) for 4 min at 25°C. Sections were dehydrated through a series of ethanol solutions, xylene, and over-slipped with Permount (Fisher Scientific, Waltham, MA, USA). Sections were then analyzed using a BZ-8000 microscope with BZ Image Measurement Software (KEYENCE, Osaka, Japan).

Immunohistochemical analysis

To perform fluorescence immunohistochemistry, retinal sections were washed with 0.1 M K^+-free PBS and incubated with 50% methanol followed by 100% methanol for 10 min. Following treatment with blocking buffers [bovine serum albumin (BSA) as well as 10% goat serum with 0.1% Triton X-100 in phosphate buffered saline (PBST)], retinal sections were incubated overnight at 4°C with following primary antibodies: anti-NeuN (1 : 100; mouse monoclonal IgG_1, clone A60; Chemicon, Temecula, CA, USA); anti-syntaxin-1 (1 : 500; mouse monoclonal; Sigma-Aldrich, St. Louis, MO, USA); and anti-Chx10 (1 : 300; sheep polyclonal; Exalpha Biologicals Inc., MA, USA). Sections were then incubated with Alexa Fluor 488-conjugated anti-mouse IgG and Alexa Fluor 488-conjugated anti-sheep IgG secondary antibodies (1 : 300; Molecular Probes, Eugene, OR, USA). The nuclei were visualized with Hoechst 33342 (1 : 10 000; Molecular Probes). Samples were then washed thoroughly with PBS and cover-slipped with Perma Fluor (Thermo Shandon, Pittsburgh, PA, USA). Images were collected using a BZ-8000 microscope with BZ Image Measurement Software.

For blood vessels staining, biotinylated *Lycopersicon esculentum* (tomato) lectin (Vector Laboratories, Burlingame, CA, USA) is diluted with PBS. Biotinylated tomato lectin was injected (1 mg/mL, 100 μL, i.v.) at 24 h after cerebral ischemia (1 h tMCAO). Mice were perfused 5 min after tomato lectin injection. Following tissue preparation as described in the method section, coronal brain section was blocked with 2% BSA in 0.1% PBST for 2 h, and then incubated with Alexa Fluor 488 streptavidin conjugates for 2 h at 25°C. Sections were washed with PBS and cover-slipped with Perma Fluor. Images were collected using an LSM 710 confocal microscope with ZEN Software (Carl Zeiss, Oberkochen, Germany).

TTC staining

For 2,3,5–triphenyltetrazolium chloride (TTC) staining, brain was quickly removed at 24 h after cerebral ischemia (1 h tMCAO)

followed by P_{30} administration ($n = 7$), sectioned coronally with a 1-mm thickness and washed with K^+-free PBS. Brain slices were incubated in 2% TTC (Sigma-Aldrich) in 0.9% NaCl in dark place for 15–20 min at 25°C and transferred in 4% PFA overnight. Images of brain slices were then collected by scanner, and infarct volume was calculated by Image J software (NIH, Bethesda, MD, USA).

Behavioral assessments

Following P_{30} administration with doses of 0.03 and 3 nmol/5 μL (i.c.v., $n = 6$ and $n = 7$, respectively), 0.3 and 1 mg/kg (i.v., $n = 5$ and $n = 7$, respectively) at 1 h as well as 1 mg/kg (i.v.) at 3 and 6 h ($n = 5$ and $n = 7$, respectively) after cerebral ischemia (1 h tMCAO), behavioral studies were assessed through 14 days. Clinical score was evaluated from day 1 after ischemia in the following way: 0, no observable deficits; 1, failure to extend the forepaw fully; 2, circling; 3, falling to one side; 4, no spontaneous movement; 5, death. In this study, 0.5 point was added to each score when the motor dysfunction was severe for scores between 1 and 4. Survival rate was evaluated from day 1 after tMCAO and calculated by the percentage of vehicle or P_{30} post-treated mice that were alive through 14 days after ischemia.

Statistical analysis

All results are shown as means ± SEM. Two independent groups were compared using the Student's *t*-test. Multiple groups were compared using Dunnett's multiple comparison test after a one-factor ANOVA or a repeated measure ANOVA. Survival rate was compared using Logrank test after Kaplan–Meyer method. $p < 0.05$ was considered significant.

Results

Characterization of functionally active core peptide in ProTα

The functionally active core domain in rat recombinant ProTα was determined by measuring the survival activity of cultured cortical neurons in the presence of different deletion mutants of GST-fusion ProTα at 12 h after the ischemic (serum-free) stress (Fig. 1a–c). The findings revealed that the N-terminal deletion mutants ProTα (Δ1–29 and Δ1–48) as well as C-terminal deletion mutants ProTα (Δ79–112 and Δ102–112) elicit its protective effect as like as full-length ProTα against ischemic stress-induced cultured neuronal damages (Fig. 1b, c). However, the deletion mutants of ProTα devoid of central peptide sequence comprised of 30 amino acids (P_{30}: a.a. 49–78) abolished its neuroprotective activity against the ischemic stress (Fig. 1b, c). Interestingly, the core peptide sequence P_{30} (a.a. 49–78) itself exerted the full survival effect in cultured neurons against ischemic damages, an indication of neuroprotective characteristics of ProTα-derived peptide P_{30} (Fig. 1b, c).

Blockade of retinal ischemia-induced damages by ProTα-derived peptides

We reported previously that ProTα inhibits the retinal ischemia-induced functional and cellular damages (Fujita *et al.* 2009). To evaluate whether ProTα-derived peptide has protective activity against ischemic damages *in vivo*, P_{30} was injected (i.vt.) with doses of 1, 3 and 10 pmol/μL in the

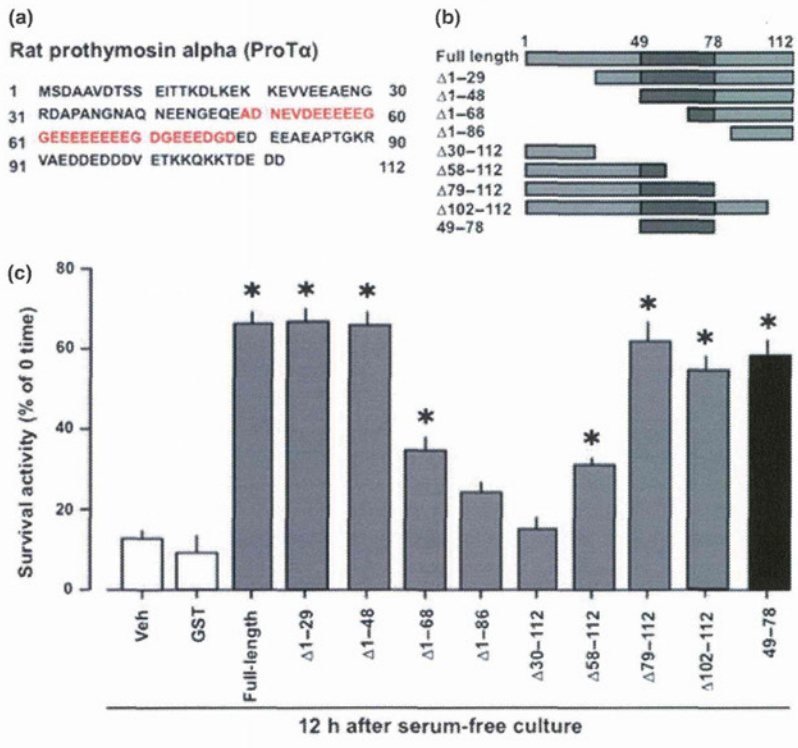

Fig. 1 The central core peptide sequence of prothymosin alpha (ProTα) is an essential domain for survival activity of ProTα against serum-free ischemic stress. (a) The amino acid sequence of rat ProTα. Red colored sequence indicates functional core domain (a.a. 49–78 referred as P_{30}) in ProTα. (b) Schematic drawings of GST-fusion of full length ProTα and its deletion mutants. (c) Identification of essential domain of ProTα for its survival activity. The primary cultured cortical neurons were incubated with GST and GST-fusion ProTα mutants under the serum-free condition. The survival activity was measured at 12 h after the start of culture. Data represent the means ± SEM. (*$p < 0.01$, vs. Veh).

ipsilateral eye at 24 h after retinal ischemia. The hematoxylin and eosin (H&E) staining data showed that the number of cells in different retinal layers as well as the retinal thickness is significantly decreased in the vehicle-treated mice at day 7 after the ischemic stress, whereas 10 pmol P_{30} maximally and significantly inhibited this cellular loss in retina and decrease in retinal thickness at day 7 (Fig. 2a, b).

In electroretinogram (ERG), the amplitude called a-wave represents the functional activity of photoreceptor cells, whereas b-wave indicates the functions of mixture of cells including bipolar, Muller, amacrine, and ganglion cells (Asi and Perlman 1992; Fujita *et al.* 2009). Following after retinal ischemia and reperfusion, the ERGs analysis showed that a- and b-wave amplitudes are significantly decreased in the vehicle-treated mice at day 7 after retinal ischemia, compared with the control (Fig. 2c, d). Following P_{30} treatment, dose-dependent increase in a- and b-wave amplitudes were observed at day 7 after the retinal ischemic stress, and 10 pmol P_{30} exerted its maximum protective effect against the ischemic damages (Fig. 2c, d). On the other hand, no significant protective effect of thymosin alpha 1 (a.a. 2–29) corresponding to N-terminal sequence of ProTα and the C-terminal peptide (a.a. 102–112) against retinal ischemic damages were observed at day 7 after ischemia (data are not shown).

P_{30}-induced cell type-specific survival against retinal ischemic damages

To examine the cell type-specific protective activity of ProTα-derived peptide in ischemic retina, P_{30} was injected (10 pmol/μL, i.vt.) in the ipsilateral eye at 24 h after retinal ischemia. The immunohistochemical analysis showed that NeuN-positive neurons (Buckingham *et al.* 2008) in the ganglion cell layer (GCL) are significantly diminished at day 7 after retinal ischemic stress, compared to the control (Fig. 3a). Following P_{30} treatment at 24 h after retinal

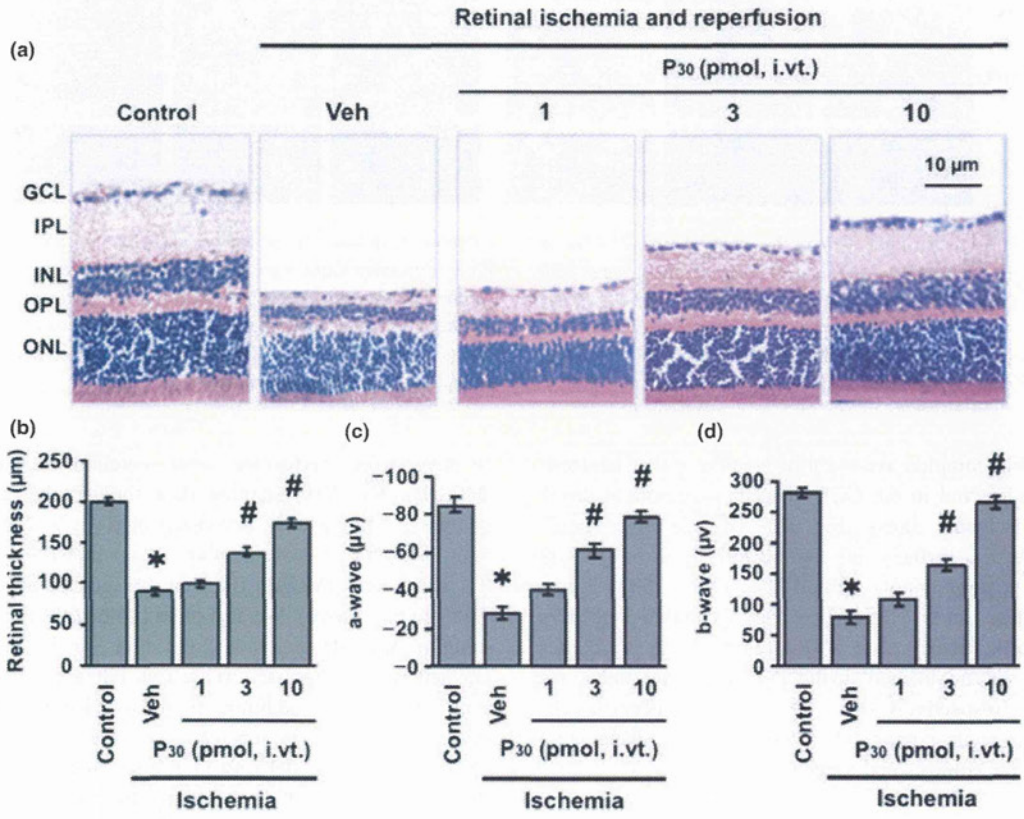

Fig. 2 Prothymosin alpha (ProTα)-derived peptide protects the retinal ischemia-induced functional damages. P_{30} is injected intravitreously (i.vt.) at the doses of 1, 3, and 10 pmol/μL in the ipsilateral eye at 24 h after retinal ischemia. Vehicle is treated with 0.05% dimethyl sulfoxide (DMSO) in a similar manner. (a–d) Protective activity of P_{30} is a dose-dependent manner. Following P_{30} injection at 24 h after retinal ischemia, (a) hematoxylin and eosin (H&E) staining of retinal section is performed at day 7 (right panel). (b–d) Measurement of retinal thickness (b) as well as the a-wave (c) and b-wave (d) amplitudes of ERG analysis are done at day 7 after retinal ischemia in P_{30} post-treated mice. Data are mean ± SEM. (*$p < 0.05$, vs. Control, #$p < 0.05$, vs. Veh) from experiments using five to seven mice for each group.

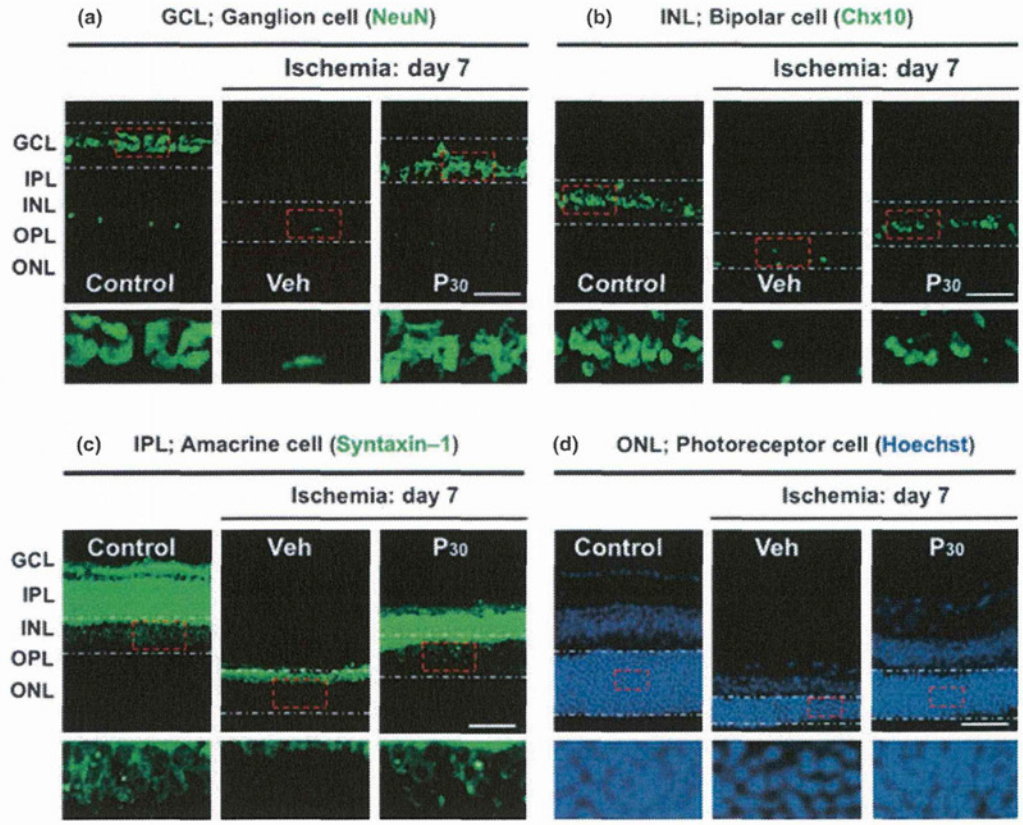

Fig. 3 Cell type-specific protection by P_{30} against retinal ischemic damages. P_{30} is injected (10 pmol/μL; i.vt.) in the ipsilateral eye at 24 h after retinal ischemic stress, and the immnunohistochemical analysis of retinal sections is performed at day 7. (a–d) The staining of ganglion cells (a) in the ganglion cell layer (GCL) (NeuN: green), bipolar cells (b) in the inner nuclear layer (INL) (Chx10: green), amacrine cells (c) (syntaxin–1: green), photoreceptor cells (d) in the outer nuclear layer (ONL) (Hoechst: blue) are done at day 7 after retinal ischemia. The higher magnification views of lower panels in (a–d) indicate the expression of retinal cell types noted by dotted rectangles (respective upper panels). Scale bars: 10 μm. Experiments were performed using five to eight mice for each group.

ischemia, the complete recovery of NeuN-positive neuronal cells was observed in the GCL of ischemic retina at day 7 after the ischemic stress (Fig. 3a). On the other hand, treatment of P_{30} partially, but significantly blocked the loss of Chx10-positive bipolar cells (Rhee *et al.* 2007) in the inner nuclear layer (INL) (Fig. 3b), syntaxin-1-positive amacrine cells (Sherry *et al.* 2006), of which the cell bodies and processes are located in the INL and inner plexiform layer (IPL), respectively (Fig. 3c), and photo-receptor cells in the outer nuclear layer (ONL) (Fig. 3d), compared with the respective controls and vehicles.

Inhibition of cerebral ischemia-induced brain damages by P_{30}

To evaluate the protective activity of P_{30} against ischemic brain damages, mice were post-treated with P_{30} in time- and dose-dependent manner following different routes of administration, and subsequent 2,3,5-triphenyl tetrazolium chloride (TTC) staining at 24 h and behavioral assessments through 14 days were performed after cerebral ischemia (1 h tMCAO). The TTC staining data showed that the infarct volume is significantly decreased at 24 h in the ischemic brain by intracerebroventicular (i.c.v.) injection of 3 nmol P_{30} at 1 h after tMCAO (Fig. 4a, b), but not by 0.03 nmol (data are not shown). We also observed that the clinical score is significantly decreased at day 1 after 1 h tMCAO in mice injected with 3 nmol P_{30} (i.c.v.) at 1 h after the ischemic stress (Fig. 4c). In addition, significant decrease in clinical score and increase in survival rate were observed through 14 days after i.c.v. delivery (1 h after ischemia) of 3 nmol P_{30}, an indication of long-lasting protective effect of P_{30} against ischemic brain damages (Fig. 4d, e).

On the other hand, P_{30} was injected intravenously (i.v.) with doses of 0.3 and 1 mg/kg at 1 h after cerebral ischemia (1 h tMCAO). Our TTC staining data revealed that the infarct volume is significantly decreased at 24 h in the ischemic brain treated with 1 mg/kg of P_{30} treatment at 1 h after the ischemic stress (Fig. 4f, g). Following

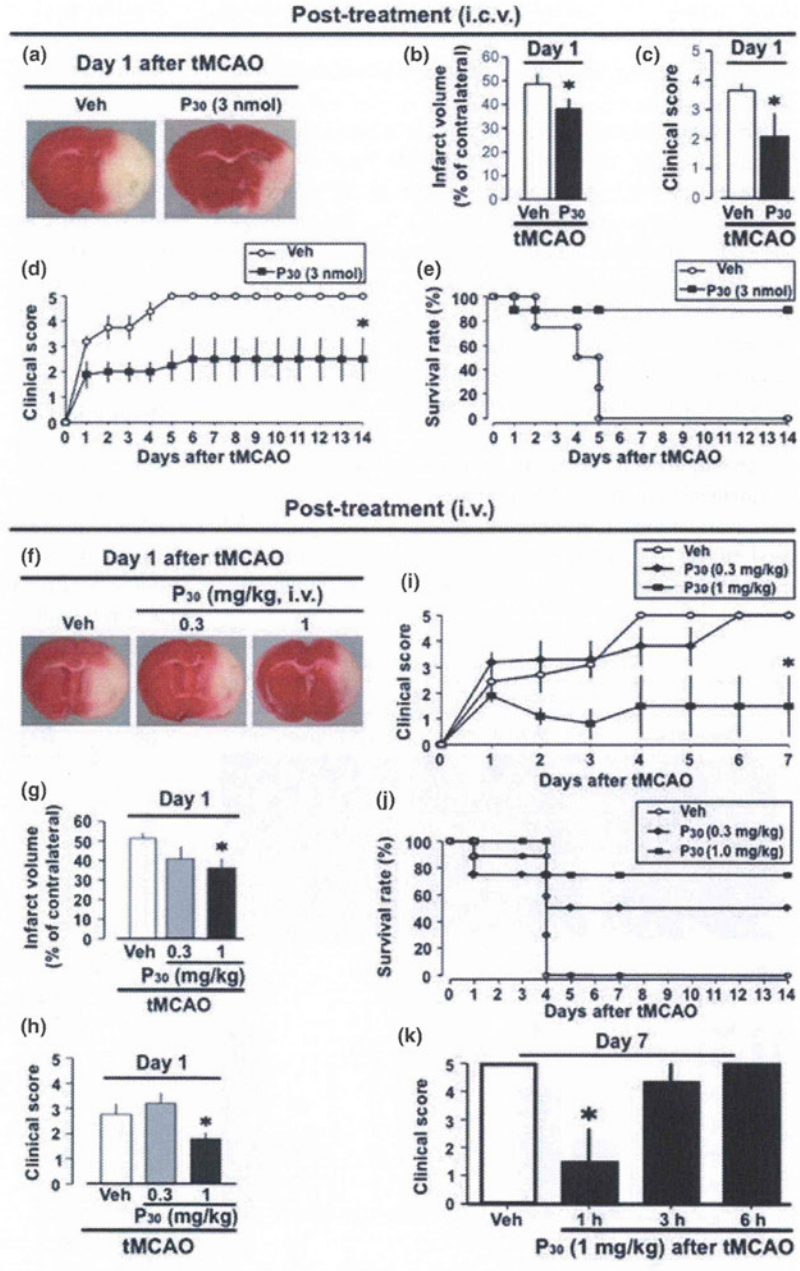

Fig. 4 P_{30} inhibits cerebral ischemia-induced brain damages. (a–e) Intracerebroventricular (i.c.v.) delivery with P_{30} protects ischemic brain damages. P_{30} is injected (3 nmol, i.c.v.) in the brain at 1 h after the cerebral ischemia [1 h transient middle cerebral artery occlusion (tMCAO)], (a–c) TTC staining (a), measurement of infarct volume (b), and clinical scores (c) are performed at day 1 after tMCAO. Data represent the means ± SEM. (*$p < 0.05$, vs. Veh). (d, e) Assessment of the clinical score (d) and survival rate (e) are done through 14 days after the tMCAO mice post-treated with P_{30}. The group of P_{30} treatment was significant compared to group of Veh treatment (*$p < 0.01$, vs. Veh). Survival rate of P_{30} treatment tended to be significant compared to Veh treatment. Experiments were performed using five to eight mice for each group. (f–k) Blockade of cerebral ischemia-induced brain damages by systemic administration of P_{30}. P_{30} is delivered intravenously (i.v.) with doses of 0.3 and 1 mg/kg at 1 h after cerebral ischemia (1 h tMCAO). (f–h) TTC staining (f), measurement of infarct volume (g) and clinical scores (h) are performed at day 1 after tMCAO. (i, j) The clinical score (i) and survival rate (j) are measured for 7 and 14 days, respectively. The group of P_{30} treatment (1 mg/kg) was significant compared to group of Veh treatment in clinical score (*$p < 0.01$, vs. Veh). Survival rate of P_{30} treatment tended to be significant compared to Veh treatment. (k) Time-course systemic injection of P_{30} (1 mg/kg, i.v.) at 1, 3, and 6 h after cerebral ischemia (1 h tMCAO). Data represent the means ± SEM. (*$p < 0.05$, vs. Veh). Experiments are performed using six to eight mice for each group.

post-treatment (i.v.) with 1 mg/kg of P_{30} at the same time point, the clinical score was significantly declined through 7 days and survival rate was maximally increased through 14 days after tMCAO, compared with the vehicle and ischemic mice treated with 0.3 mg/kg of P_{30} (Fig. 4h–j). The behavioral study also confirmed that systemic (i.v.) P_{30} delivery with the dose of 1 mg/kg at 1 h after ischemia induces it maximum protective effect at day 7 against the ischemic brain damages, compared to P_{30} treatment at 3 or 6 h after cerebral ischemia (Fig. 4k).

P_{30} inhibits the cerebral ischemia-induced blood vessel damages

In the ischemic stroke and cerebrovascular disease, vascular defect is occurred along with neuronal damages (Paul *et al.* 2001; Fujita and Ueda 2007). To investigate whether P_{30} protects the ischemia-induced blood vessels damages, P_{30} was injected (1 mg/kg; i.v.) at 1 h after cerebral ischemia (1 h tMCAO). Following blood vessel immunostaining using biotinylated tomato lectin and Alexa Fluor 488 streptavidin at 24 h after ischemia, the findings revealed that the number

blood vessels are markedly decreased in somatosensory cortex in the brain of vehicle-treated mice, compared with the control (Fig. 5a, b). In addition, the decrease in lengths of the blood vessels was observed at 24 h after tMCAO (Fig. 5a, c). This ischemia-induced loss of tomato lectin-stained blood vessels in terms of number and lengths was completely recovered in the somatosensory cortex at 24 h after the ischemic stress in mice post-treated with P_{30}, but the lengths were relatively larger than the vessels in the control brain, an indication of the protective role of P_{30} against ischemia-induced blood vessel damages (Fig. 5a–c). Similar results of the recovery of cerebral ischemia-induced blood vessels damages by P_{30} were observed in the striatum and hippocampus at 24 h after 1 h tMCAO (data are not shown).

P_{30} ameliorates the ischemic brain caused by photochemically induced thrombosis

It is well known that ischemic model because of middle cerebral artery (MCA) occlusion with photochemically induced thrombosis (PIT) is analogous to clinical condition (Tanaka *et al.* 2007). In this ischemic mouse model, there was a significant behavioral damage evaluated by clinical score (Fig. 6a). This damage was significantly attenuated by systemic post-treatment with P_{30} (1 mg/kg, i.v.) at 1 h after PIT (Fig. 6a). Following behavioral study after PIT stress, neurological assessments using TTC staining were performed at 24 h. The TTC staining data revealed that there was a marked increase in cerebral infarction observed at 24 h after PIT in vehicle-treated mice (Fig. 6b), but this cerebral brain damage in terms of infarct volume and hemisphere expansion was significantly inhibited by systemic treatment of P_{30} (Fig. 6c, d).

Discussion

This study demonstrates three major findings. First, active core peptide domain P_{30} (a.a. 49–78) derived from ProTα retains the original survival activity in cultured neuronal cells against ischemic (serum-free) stress. Second, characterizations of P_{30} actions reveal that it potently inhibits the ischemia-induced damages in retina and brain. Third, P_{30}

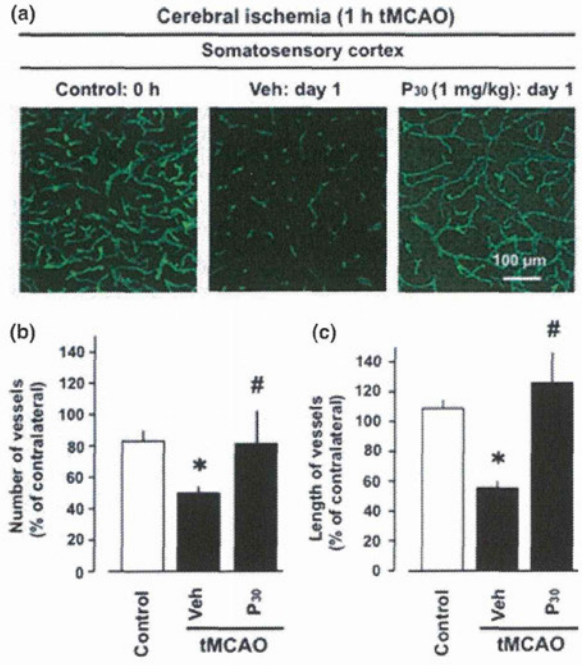

Fig. 5 P_{30} inhibits the cerebral ischemia-induced blood vessels damages. (a–c) P_{30} is injected (1 mg/kg, i.v.) at 1 h after cerebral ischemia [1 h transient middle cerebral artery occlusion (tMCAO)]. Following administration with biotinylated tomato lectin (1 mg/mL, 100 μL, i.v.) at 24 h after cerebral ischemia (1 h tMCAO), and subsequent perfusion 5 min after biotinylated tomato lectin injection, immunostaining of blood vessels by Alexa Fluor 488 streptavidin (a) as well as measurement of number (b) and length (c) of blood vessels is performed at day 1 after the ischemic stress. Data represent the means ± SEM. (*$p < 0.05$, vs. Control, #$p < 0.05$, vs. Veh) from experiments using five to seven mice for each group.

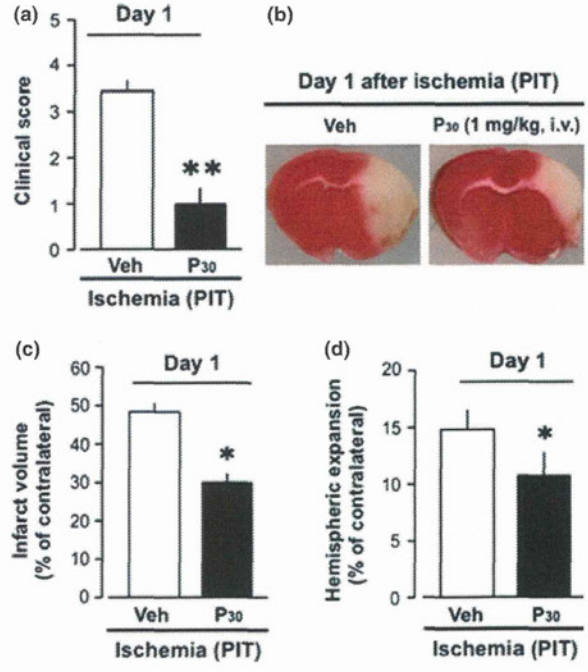

Fig. 6 P_{30} improves the ischemic brain damages caused by photochemically induced thrombosis. P_{30} is administered (1 mg/kg, i.v.) at 1 h after photochemically induced thrombosis (PIT) in mice. (a) Clinical scores at day 1 after ischemia. (b) Representative picture of TTC staining at 24 h after PIT. (c, d) Measurement of infarct volume (c) and hemispheric expansion (d) at 24 h after PIT. Data represent the means ± SEM. (*$p < 0.05$, **$p < 0.01$, vs. Veh) from experiments using five to seven mice for each group.

induces protective action against ischemia-induced disruption of cerebral blood vessels.

Several *in vitro* studies reported about the different sequence-specific functions of ProTα, which is also involved in the mechanisms of cell survival (Jiang *et al.* 2003; Karapetian *et al.* 2005; Skopeliti *et al.* 2007; Ueda *et al.* 2007; Ueda 2009; Mosoian *et al.* 2010; Danielli *et al.* 2012; Dong *et al.* 2012). On the basis of previous information, we firstly designed *in vitro* experiments to find out the sequence-specific neuroprotective actions of ProTα using various deletion mutants of GST-ProTα in neuronal cells culture under ischemic stress. The peptides lacking sequence (a.a. 1–29), which belongs to thymosin alpha 1 (a.a. 2–29), sequence (a.a. 1–48), which mostly covers the binding region for Keap1, or C-terminal sequences (a.a. 79–112 and 102–112) completely retained the original survival activity as like ProTα. However, the significant decrease in survival effect was observed by the deficiency of parts of the central core peptide sequence comprised of 30 amino acids in ProTα (a.a. 49–78). Interestingly, this central active core peptide of ProTα referred as P_{30} (a.a. 49–78) itself exerts full survival action in neuronal cells against ischemia. Retinal ischemia causes the functional and cellular damages in different layers of retina through several destructive cascade of mechanisms, as consequence of visual impairment and blindness (Osborne *et al.* 2004). Our recent *in vivo* studies suggested that ProTα potently inhibits this ischemia-induced functional and cellular damages of retina (Fujita *et al.* 2009; Ueda *et al.* 2010). To evaluate the *in vivo* protective effect of P_{30} against ischemic damages, ischemic retina was post-treated with P_{30}. The findings using H&E staining and ERG study revealed that P_{30} significantly blocks the retinal ischemia-induced decrease in cells number of different layers and retinal thickness. In addition, immunohistochemical analysis clarified that P_{30} completely rescues the retinal ischemia-induced ganglion cell damages, along with the partial but significant blockade of the loss of bipolar, amacrine, and photoreceptor cells. Stroke following cerebral ischemia (tMCAO) or photothrombotic brain ischemia causes the neuronal damages, along with adequate disruption of cerebral blood vessels (Beck and Plate 2009; Hofmeijer and van Putten 2012; Krysl *et al.* 2012). We previously explained the protective role of ProTα against cerebral ischemia-induced brain damages (Fujita and Ueda 2007; Ueda 2009; Ueda *et al.* 2010). The present findings of TTC staining and neurological assessment suggested that intracerebroventicular (3 nmol, i.c.v.) or systemic (1 mg/kg, i.v.) treatment with P_{30} at 1 h after cerebral ischemia (1 h tMCAO) significantly blocks ischemia-induced brain damages. Following immunostaining with tomato lectin in P_{30}-treated (1 mg/kg, i.v.) ischemic mice, the complete recovery of ischemia-induced (tMCAO) cerebral blood vessels damages was observed through day 1, a consideration of P_{30} as a new angiogenic factor. In addition, systemic administration with P_{30} (1 mg/kg, i.v.) significantly ameliorated the ischemic brain caused by photochemically induced thrombosis (PIT), a representative clinical model of cerebral ischemia.

The present investigations were performed following several routes of the administration of P_{30}. According to the fact that retinal ischemia possesses high reproducibility and quantitation to understand the pathophysiological changes and signaling pathways under ischemic condition (Prasad *et al.* 2010), we used this ischemic injury as a simple model for screening of survival activity by i.vt. administration of P_{30}. We already reported that i.v. administration with full-length ProTα induces protective effect against retinal ischemia (Fujita *et al.* 2009). In brain ischemia, we firstly decided to perform i.c.v. administration of P_{30} to evaluate the improvement of ischemic injury, and successfully confirmed against ischemic brain damages. Our recent studies revealed that myc-tagged ProTα (1 mg/kg) is penetrated to the damaged area of brain at least 3 h after brain ischemia by intraperitoneal (i.p.) administration, and that systemic administration (i.p. and i.v.) of ProTα ameliorates brain ischemia-induced functional and cellular damages (Fujita and Ueda 2007). It is well known that brain ischemic stress disrupts the blood–brain barrier (BBB) (Paul *et al.* 2001; Fujita and Ueda 2007). Thus, we presume that like ProTα, systemic administrated P_{30} would penetrate to the damaged brain through the disrupted BBB. Although relationship between route of administration and penetrated amounts of P_{30} to the brain are not clear, isotope and/or fluorescence labeling might be useful method for the calculation of penetration. In the systemic administration, ProTα and P_{30} exercise the maximum improvement effect against brain ischemia in 100 μg/kg (equivalent 8.08 nmoles/kg) and 1 mg/kg (equivalent 0.30 μmoles/kg), respectively. This difference of efficacy between ProTα and P_{30} might be because of the stability of P_{30} *in vivo*, though GST-ProTα and GST-P_{30} (a.a. 49–78) showed similar survival activity in this *in vitro* study. However, the modification of amino acid and/or mutation in sequence of P_{30} may provide a better solution to improve the stability and survival activity of P_{30}. This should be the next issue to address.

Cortical neurons in serum-free primary culture rapidly die by necrosis, which is completely inhibited by ProTα (Fujita and Ueda 2003; Ueda *et al.* 2007). As ProTα also protects the retinal ischemia-induced necrosis and apoptosis through the up-regulation of BDNF and EPO, and this retinal protection is completely abolished by antisense oligodeoxynucleotide or antibody treatment against ProTα (Fujita *et al.* 2009; Ueda *et al.* 2010), it should be an interesting next subject to investigate whether the same mechanisms are involved in the P_{30}-induced functional and cellular protection against ischemic damages. Despite of being neuroprotective activity of several proteins, peptides have been detected as a new class of attractable therapeutic molecule owing to their diversity, synthesis, and higher

capability to penetrate the challenging targets (Archakov *et al.* 2003; Watt 2006; Gozes 2007; Patel *et al.* 2007; Meade *et al.* 2009). Taken together, this study confers a precise demonstration about the broad-spectrum protective activity of ProTα-derived small peptide P_{30} against ischemic damages *in vitro* and *in vivo*. Thus, it is evident that P_{30} mimics the *in vitro* and *in vivo* neuroprotective actions of ProTα. The sequence homology of P_{30} domain in ProTα among all species is highly conserved; furthermore, this sequence is completely equal in human, rat, and mouse. From these facts, it is speculated that P_{30} domain may plays important roles in robustness of ProTα against neuronal damages.

In conclusion, ProTα-derived peptide P_{30} exerted its survival actions in cultured neurons against ischemic stress. P_{30} significantly blocked the ischemia-induced functional and cellular damages in retina as well as in brain, along with inhibition of the cerebral blood vessels disruption. Therefore, detailed mechanisms underlying neuroprotection by ProTα-derived small peptide may provide a novel therapeutic approach for the treatment of ischemic damages in the central nervous system.

Acknowledgements

We thank R. Fujita, J. Sugimoto, and S. Maeda for technical assistance and advice. We also thank M. Moskowitz for the valuable discussion. We acknowledge Parts of this study were supported by Grants-in-Aid for Scientific Research (to H.U.) from the Ministry of Education, Culture, Sports, Science and Technology (MEXT), and Health and Labor Sciences Research Grants (to H.U.) on Research from the Ministry of Health, Labor and Welfare. We have no conflict interest to report.

References

Archakov A. I., Govorun V. M., Dubanov A. V., Ivanov Y. D., Veselovsky A. V., Lewi P. and Janssen P. (2003) Protein-protein interactions as a target for drugs in proteomics. *Proteomics* **3**, 380–391.

Asi H. and Perlman I. (1992) Relationships between the electroretinogram a-wave, b-wave and oscillatory potentials and their application to clinical diagnosis. *Doc. Ophthalmol.* **79**, 125–139.

Beck H. and Plate K. H. (2009) Angiogenesis after cerebral ischemia. *Acta Neuropathol.* **117**, 481–496.

Bejot Y., Prigent-Tessier A., Cachia C., Giroud M., Mossiat C., Bertrand N., Garnier P. and Marie C. (2011) Time-dependent contribution of non neuronal cells to BDNF production after ischemic stroke in rats. *Neurochem. Int.* **58**, 102–111.

Blanco R. E., Soto I., Duprey-Diaz M. and Blagburn J. M. (2008) Upregulation of brain-derived neurotrophic factor by application of fibroblast growth factor-2 to the cut optic nerve is important for long term survival of retinal ganglion cells. *J. Neurosci. Res.* **86**, 3382–3392.

Buckingham B. P., Inman D. M., Lambert W., Oglesby E., Calkins D. J., Steele M. R., Vetter M. L., Marsh-Armstrong N. and Horner P. J. (2008) Progressive ganglion cell degeneration precedes neuronal loss in a mouse model of glaucoma. *J. Neurosci.* **28**, 2735–2744.

Danielli R., Fonsatti E., Calabrò L., Giacomo A. M. and Maio M. (2012) Thymosin α1 in melanoma: from the clinical trial setting to the daily practice and beyond. *Ann. N. Y. Acad. Sci.* **1270**, 8–12.

Dong G., Callegari E. A., Gloeckner C. J., Ueffing M. and Wang H. (2012) Prothymosin-α interacts with mutant huntingtin and suppresses its cytotoxicity in cell culture. *J. Biol. Chem.* **287**, 1279–1289.

Dvoriantchikova G., Barakat D. J., Hernandez E., Shestopalov V. I. and Ivanov D. (2010) Liposome-delivered ATP effectively protects the retina against ischemia-reperfusion injury. *Mol. Vis.* **16**, 2882–2890.

Feigin V. L. (2005) Stroke epidemiology in the developing world. *Lancet* **365**, 2160–2161.

Flynn R. W., MacWalter R. S. and Doney A. S. (2008) The cost of cerebral ischaemia. *Neuropharmacology* **55**, 250–256.

Fornage M. (2009) Genetics of stroke. *Curr. Atheroscler. Rep.* **11**, 167–174.

Fujita R. and Ueda H. (2003) Protein kinase C-mediated cell death mode switch induced by high glucose. *Cell Death Differ.* **10**, 1336–1347.

Fujita R. and Ueda H. (2007) Prothymosin-alpha1 prevents necrosis and apoptosis following stroke. *Cell Death Differ.* **14**, 1839–1842.

Fujita R., Ueda M., Fujiwara K. and Ueda H. (2009) Prothymosin-alpha plays a defensive role in retinal ischemia through necrosis and apoptosis inhibition. *Cell Death Differ.* **16**, 349–358.

Garaci E., Favalli C., Pica F. *et al.* (2007) Thymosin alpha 1: from bench to bedside. *Ann. N. Y. Acad. Sci.* **1112**, 225–234.

Goldstein A. L. and Goldstein A. L. (2009) From lab to bedside: emerging clinical applications of thymosin alpha 1. *Expert Opin. Biol. Ther.* **9**, 593–608.

Gozes I. (2007) Activity-dependent neuroprotective protein: from gene to drug candidate. *Pharmacol. Ther.* **114**, 146–154.

Halder S. K., Matsunaga H. and Ueda H. (2012) Neuron-specific non-classical release of prothymosin alpha, a novel neuroprotective DAMPs. *J. Neurochem.* **123**, 262–275.

Hofmeijer J. and van Putten M. J. (2012) Ischemic cerebral damage: an appraisal of synaptic failure. *Stroke* **43**, 607–615.

Iadecola C. and Anrather J. (2011) The immunology of stroke: from mechanisms to translation. *Nat. Med.* **17**, 796–808.

Jiang X., Kim H. E., Shu H. *et al.* (2003) Distinctive roles of PHAP proteins and prothymosin-alpha in a death regulatory pathway. *Science* **299**, 223–226.

Karapetian R. N., Evstafieva A. G., Abaeva I. S. *et al.* (2005) Nuclear oncoprotein prothymosin alpha is a partner of Keap1: implications for expression of oxidative stress-protecting genes. *Mol. Cell. Biol.* **25**, 1089–1099.

Korada S., Zheng W., Basilico C., Schwartz M. L. and Vaccarino F. M. (2002) Fibroblast growth factor 2 is necessary for the growth of glutamate projection neurons in the anterior neocortex. *J. Neurosci.* **22**, 863–875.

Krysl D., Deykun K., Lambert L., Pokorny J. and Mares J. (2012) Perifocal and remote blood-brain barrier disruption in cortical photothrombotic ischemic lesion and its modulation by the choice of anesthesia. *J. Physiol. Pharmacol.* **63**, 127–132.

Madinier A., Bertrand N., Mossiat C., Prigent-Tessier A., Beley A., Marie C. and Garnier P. (2009) Microglial involvement in neuroplastic changes following focal brain ischemia in rats. *PLoS ONE* **4**, e8101.

Maiese K., Li F. and Chong Z. Z. (2004) Erythropoietin in the brain: can the promise to protect be fulfilled?. *Trends Pharmacol. Sci.* **25**, 577–583.

Matsunaga H. and Ueda H. (2010) Stress-induced non-vesicular release of prothymosin-alpha initiated by an interaction with S100A13,

and its blockade by caspase-3 cleavage. *Cell Death Differ.* **17**, 1760–1772.

Meade A. J., Meloni B. P., Mastaglia F. L. and Knuckey N. W. (2009) The application of cell penetrating peptides for the delivery of neuroprotective peptides/proteins in experimental cerebral ischaemia studies. *J. Exp. Stroke Transl. Med.* **2**, 22–40.

Mosoian A., Teixeira A., Burns C. S., Sander L. E., Gusella L. G., He C., Blander J. M., Klotman P. and Klotman M. E. (2010) Prothymosin-α inhibits HIV-1 via Toll-like receptor 4-mediated type I interferon induction. *Proc. Natl Acad. Sci. USA* **107**, 10178–10183.

Nagai N., Van Hoef B. and Lijnen H. R. (2007) Plasminogen activator inhibitor-1 contributes to the deleterious effect of obesity on the outcome of thrombotic ischemic stroke in mice. *J. Thromb. Haemost.* **5**, 1726–1731.

Neroev V. V., Zueva M. V. and Kalamkarov G. R. (2010) Molecular mechanisms of retinal ischemia. *Vestn. oftalmol.* **126**, 59–64.

Osborne N. N., Casson R. J., Wood J. P., Chidlow G., Graham M. and Melena J. (2004) Retinal ischemia: mechanisms of damage and potential therapeutic strategies. *Prog. Retin. Eye Res.* **23**, 91–147.

Paolucci S., Antonucci G., Grasso M. G., Bragoni M., Coiro P., Angelis D. D., Morelli D., Venturiero V., Troisi E. and Pratesi L. (2003) Functional outcome of ischemic and hemorrhagic stroke patients after inpatient rehabilitation: A matched comparison. *Stroke* **34**, 2861–2865.

Patel L. N., Zaro J. L. and Shen W. C. (2007) Cell penetrating peptides: intracellular pathways and pharmaceutical perspectives. *Pharm. Res.* **24**, 1977–1992.

Paul R., Zhang Z. G., Eliceiri B. P., Jiang Q., Boccia A. D., Zhang R. L., Chopp M. and Cheresh D. A. (2001) Src deficiency or blockade of Src activity in mice provides cerebral protection following stroke. *Nat. Med.* **7**, 222–227.

Pierluigi B., D'Angelo C., Fallarino F., Moretti S., Zelante T., Bozza S., De Luca A., Bistoni F., Garaci E. and Romani L. (2010) Thymosin alpha1: the regulator of regulators?. *Ann. N. Y. Acad. Sci.* **1194**, 1–5.

Prasad S. S., Kojic L., Wen Y. H., Chen Z., Xiong W., Jia W. and Cynader M. S. (2010) Retinal gene expression after central retinal artery ligation: effects of ischemia and reperfusion. *Invest. Ophthalmol. Vis. Sci.* **51**, 6207–6219.

Rhee K. D., Ruiz A., Duncan J. L., Hauswirth W. W., Lavail M. M., Bok D. and Yang X. J. (2007) Molecular and cellular alterations induced by sustained expression of ciliary neurotrophic factor in a mouse model of retinitis pigmentosa. *Invest. Ophthalmol. Vis. Sci.* **48**, 1389–1400.

Sherry D. M., Mitchell R., Standifer K. M. and du Plessis B. (2006) Distribution of plasma membrane-associated syntaxins 1 through 4 indicates distinct trafficking functions in the synaptic layers of the mouse retina. *BMC Neurosci.* **7**, 54.

Sims N. R. and Muyderman H. (2010) Mitochondria, oxidative metabolism and cell death in stroke. *Biochim. Biophys. Acta* **1802**, 80–91.

Siren A. L., Fratelli M., Brines M. *et al.* (2001) Erythropoietin prevents neuronal apoptosis after cerebral ischemia and metabolic stress. *Proc. Natl Acad. Sci. USA* **98**, 4044–4049.

Skopeliti M., Kratzer U., Altenberend F., Panayotou G., Kalbacher H., Stevanovic S., Voelter W. and Tsitsilonis O. E. (2007) Proteomic exploitation on prothymosin alpha-induced mononuclear cell activation. *Proteomics* **7**, 1814–1824.

Skopeliti M., Iconomidou V. A., Derhovanessian E., Pawelec G., Voelter W., Kalbacher H., Hamodrakas S. J. and Tsitsilonis O. E. (2009) Prothymosin alpha immunoactive carboxyl-terminal peptide TKKQKTDEDD stimulates lymphocyte reactions, induces dendritic cell maturation and adopts a beta-sheet conformation in a sequence-specific manner. *Mol. Immunol.* **46**, 784–792.

Tanaka Y., Koizumi C., Marumo T., Omura T. and Yoshida S. (2007) Serum S100B is a useful surrogate marker for long-term outcomes in photochemically-induced thrombotic stroke rat models. *Life Sci.* **81**, 657–663.

Ueda H. (2008) Prothymosin alpha plays a key role in cell death mode-switch, a new concept for neuroprotective mechanisms in stroke. *Naunyn Schmiedebergs Arch. Pharmacol.* **377**, 315–323.

Ueda H. (2009) Prothymosin alpha and cell death mode switch, a novel target for the prevention of cerebral ischemia-induced damage. *Pharmacol. Ther.* **123**, 323–333.

Ueda H. and Fujita R. (2004) Cell death mode switch from necrosis to apoptosis in brain. *Biol. Pharm. Bull.* **27**, 950–955.

Ueda H., Fujita R., Yoshida A., Matsunaga H. and Ueda M. (2007) Identification of prothymosin-alpha1, the necrosis-apoptosis switch molecule in cortical neuronal cultures. *J. Cell Biol.* **176**, 853–862.

Ueda H., Matsunaga H., Uchida H. and Ueda M. (2010) Prothymosin alpha as robustness molecule against ischemic stress to brain and retina. *Ann. N. Y. Acad. Sci.* **1194**, 20–26.

Ueda H., Matsunaga H. and Halder S. K. (2012) Prothymosin α plays multifunctional cell robustness roles in genomic, epigenetic, and nongenomic mechanisms. *Ann. N. Y. Acad. Sci.* **1269**, 34–43.

Watt P. M. (2006) Screening for peptide drugs from the natural repertoire of biodiverse protein folds. *Nat. Biotechnol.* **24**, 177–183.

White B. C., Sullivan J. M., DeGracia D. J., O'Neil B. J., Neumar R. W., Grossman L. I., Rafols J. A. and Krause G. S. (2000) Brain ischemia and reperfusion: molecular mechanisms of neuronal injury. *J. Neurol. Sci.* **179**, 1–33.

Witmer M. T., Pavan P. R., Fouraker B. D. and Levy-Clarke G. A. (2011) Acute retinal necrosis associated optic neuropathy. *Acta Ophthalmol.* **89**, 599–607.

Yin K. J., Deng Z., Huang H., Hamblin M., Xie C., Zhang J. and Chen Y. E. (2010) miR-497 regulates neuronal death in mouse brain after transient focal cerebral ischemia. *Neurobiol. Dis.* **38**, 17–26.

Peptides 43 (2013) 68–75

Contents lists available at SciVerse ScienceDirect

Peptides

journal homepage: www.elsevier.com/locate/peptides

Therapeutic benefits of 9-amino acid peptide derived from prothymosin alpha against ischemic damages

Sebok Kumar Halder, Junya Sugimoto, Hayato Matsunaga, Hiroshi Ueda*

Department of Molecular Pharmacology and Neuroscience, Nagasaki University Graduate School of Biomedical Sciences, 1-14 Bunkyo-machi, Nagasaki 852-8521, Japan

ARTICLE INFO

Article history:
Received 19 January 2013
Received in revised form 27 February 2013
Accepted 27 February 2013
Available online 7 March 2013

Keywords:
Blood vessel
Ischemia
Neuroprotective peptide
Prothymosin alpha

ABSTRACT

Prothymosin alpha (ProTα), a nuclear protein, plays multiple functions including cell survival. Most recently, we demonstrated that the active 30-amino acid peptide sequence/P_{30} (amino acids 49–78) in ProTα retains its substantial activity in neuroprotection *in vitro* and *in vivo* as well as in the inhibition of cerebral blood vessel damages by the ischemic stress in retina and brain. But, it has remained to identify the minimum peptide sequence in ProTα that retains neuroprotective activity. The present study using the experiments of alanine scanning suggested that any amino acid in 9-amino acid peptide sequence/P_9 (amino acids 52–60) of P_{30} peptide is necessary for its survival activity of cultured rat cortical neurons against the ischemic stress. In the retinal ischemia-perfusion model, intravitreous injection of P_9 24 h after ischemia significantly inhibited the cellular and functional damages at day 7. On the other hand, 2,3,5-triphenyltetrazolium chloride (TTC) staining and electroretinogram assessment showed that systemic delivery with P_9 1 h after the cerebral ischemia (1 h tMCAO) significantly blocks the ischemia-induced brain damages. In addition, systemic P_9 delivery markedly inhibited the cerebral ischemia (tMCAO)-induced disruption of blood vessels in brain. Taken together, the present study provides a therapeutic importance of 9-amino acid peptide sequence against ischemic damages.

1. Introduction

Ischemic stress in brain and retina causes common expression of cellular and functional damages, which include diverse injury-related cascades underlying necrosis and apoptosis, along with subsequent production and secretion of different cytotoxic mediators [7–10,21,31,34,40,44,51–53]. In addition to the release of cell-damaging mediators, some neuroprotective molecules, such as brain-derived neurotrophic factor, fibroblast growth factor and erythropoietin are simultaneously elevated after the onset of ischemia, and cause limited amelioration of ischemic injury through an inhibition of apoptosis, but not necrosis, a key mechanism of cell death [3,4,13,25,28,29,41,44,48]. Hence, it is essential to develop neuroprotective agents that target the mechanism of necrosis under ischemic condition.

We previously identified prothymosin alpha (ProTα) as a necrosis-inhibitory factor in the conditioned medium of serum-free primary culture of cortical neurons [11,45]. It has been clarified that ProTα inhibits ischemia-induced damages in brain and retina through blockade of necrosis and apoptosis [12,13,46,48]. Several studies established a relationship between ProTα and cell survival [1,23,27,30,47,49,50], and distinct amino acid sequences in ProTα are separately involved in this survival phenomenon [6,24,43]. Among them, the peptide sequence (amino acids 32–52) of the central domain in ProTα participates in the cell defensive mechanisms against oxidative stress through an interaction with Nrf2–Keap1 inhibitory complex [18,24,33]. The N-terminal sequence in ProTα (amino acids 2–29), corresponding to thymosin alpha 1, shows anti-cancer activity and induces immunodefensive action against viral infections [5,14,15,36], whereas C-terminal sequence (amino acids 89–109, 99–109 and 100–109) of human ProTα is involved in the induction of pro-inflammatory activity through toll-like receptor signaling and dendritic cell maturation [42,43]. Recently, the cell survival action of mid part (amino acids 41–83) in human ProTα against mutant huntingtin-caused cytotoxicity has been discussed [6]. Most recently, we reported that active core peptide sequence comprised of 30 amino acids (P_{30}: amino acids 49–78) in ProTα exerts its full survival effect in cultured cortical neurons against the ischemic stress and potently blocks the ischemia-induced cellular and functional damages in brain and retina and reverses the damage of cerebral blood vessels in the *in vivo* studies using various ischemic models [17]. However, it is interesting to be investigated which peptide sequence with

Abbreviations: ERG, electroretinogram; GCL, ganglion cell layer; H&E, hematoxylin and eosin; INL, inner nuclear layer; IPL, inner plexiform layer; i.v., intravenously; i.vt., intravitreously; ONL, outer nuclear layer; OPL, outer plexiform layer; ProTα, prothymosin alpha; tMCAO, transient middle cerebral artery occlusion; TTC, 2,3,5-triphenyltetrazolium chloride.

* Corresponding author. Tel.: +81 95 819 2421; fax: +81 95 819 2420.
E-mail address: ueda@nagasaki-u.ac.jp (H. Ueda).

0196-9781/$ – see front matter © 2013 Elsevier Inc. All rights reserved.
http://dx.doi.org/10.1016/j.peptides.2013.02.022

minimum amino acids of P_{30} peptide in ProTα is responsible for neuroprotection. In the present study, we evaluated the neuroprotective effect of 9-amino acid peptide derived from ProTα against the ischemic stress.

2. Materials and methods

2.1. Animals

Male C57/BLJ mice weighing 20–25 g were purchased from Tagawa Experimental Animals (Nagasaki, Japan) and used for all the experiments. Mice were kept in a room maintained at constant temperature (21 ± 2 °C) and relative humidity (55 ± 5%) with an automatic 12 h light/dark cycle with free access to standard laboratory diet and tap water. Animal care and all experimental procedures were formally approved by Nagasaki University Animal Care and Use Committee (Animal Experiments Approval Number: 1104190914).

2.2. Determination of short peptide by alanine scanning

The procedure for the identification of neuroprotective peptide sequence P_{30} (P_{30}: amino acids 49–78) in ProTα has been described previously [17]. To design ProTα-derived shorter neuroprotective peptide, alanine scanning of P_{30} was performed to determine the contribution of specific amino acid residues that retain the original function of P_{30} peptide. Neuroprotective activity of primary cultured cortical neurons was measured at 12 h after the start of serum-free culture in the presence or absence of various peptides. Cultures and methods of the measurement of survival activity were previously described [17,45].

2.3. Peptide administration

Peptide P_9 was dissolved in 0.05% dimethyl sulfoxide (DMSO), which was diluted with 0.1 M potassium (K^+)-free phosphate buffered saline (PBS). Following the protocol of injection in the eye as described previously [17], P_9 was administered intravitreously (i.vt.) with doses of 1, 3 and 10 pmol/μl at 24 h after retinal ischemia ($n = 5$, $n = 7$ and $n = 7$, respectively). On the other hand, P_9 was injected intravenously (i.v.) with doses of 0.1, 0.3 and 1 mg/kg ($n = 5$, $n = 6$, and $n = 7$, respectively) 1 h after the cerebral ischemia (tMCAO). Vehicles were treated with equal volume of 0.05% DMSO in similar manners.

2.4. Ischemic models

Two types of *in vivo* ischemic models were used throughout the experiments. Retinal ischemia was performed following the method as described previously [13,17]. Briefly, mice were anesthetized with an intraperitoneal (i.p.) injection of sodium pentobarbital (50 mg/kg) and pupils were fully dilated with 1% atropine sulfate drops (Nitten, Nagoya, Japan). The anterior chamber of the eye was cannulated with a 33-gauge needle attached to an infusion container of sterile intraocular irrigating solution (BSS PLUS dilution buffer, Alcon, Fort Worth, TX, USA). Retinal ischemia was induced by elevating the IOP to generate a hydrostatic pressure of 130 mm Hg for 45 min by lifting the container. Following 45 min after retinal ischemic stress, the needle was withdrawn and 0.3% ofloxacin (Santen Pharmaceutical Co. Ltd., Osaka, Japan) was applied topically into the eye to avoid infection.

Another ischemic model is a transient middle cerebral artery occlusion (tMCAO) model, which was induced following the method as described previously [16]. Briefly, mice were anesthetized by 2% isoflurane (Mylan, Tokyo, Japan), and body temperature was monitored and maintained at 37 °C during surgery. After a midline neck incision, the middle cerebral artery was occluded transiently using 8-0 in size monofilament nylon surgical suture (Natsume Co. Ltd., Tokyo, Japan) coated with silicon (Xantopren, Bayer dental, Osaka, Japan) that was inserted through the left common carotid artery and advanced into the left internal carotid artery. Following 1 h tMCAO, the animals were briefly re-anesthetized with isoflurane and the monofilament was withdrawn for reperfusion studies. As the silicon-coated nylon suture also plugs the branch from middle cerebral artery to supply blood to hippocampus in mice, due to small brain size, the ischemia-induced brain damages are also observed in the hippocampus. Cerebral blood flow was monitored by laser Doppler flowmeter (ALF21, Advance Co., Tokyo, Japan) using a probe (diameter 0.5 mm) of a laser Doppler flowmeter (ALF2100, Advance Co., Tokyo, Japan) inserted into the left striatum (anterior: −0.5 mm, lateral: 1.8 mm from Bregma; depth: 4.2 mm from the skull surface) through a guide cannula.

2.5. Electroretinogram

Electroretinogram (ERG) study was performed following the protocol as previously described [13,17]. Briefly, mice were dark-adapted for 3–4 h, then anesthetized with intraperitoneal injection of pentobarbital sodium (50 mg/kg) and pupils were dilated with 1% atropine. A contact electrode (KE-S, Kyoto contact lenses, Kyoto, Japan) was placed topically on the corneal apex and reference electrode was placed near the ipsilateral eye. The ground was a subdermal platinum needle electrode near the abdominal area. ERGs were produced by 20 J flash intensities. The flash stimulus source (SLS-3100, Nihon Kohden, Tokyo, Japan) illuminated the eye by diffuse reflection off the interior surface of the ganzfeld. Maximum flash luminance was measured with detector (MEB-9104, Nihon Kohden, Tokyo, Japan). After the intensity series, an incandescent background light sufficient to desensitize the rod system was turned on, and ERGs produced by the standard stimulus were recorded every 2 min for 20 min. The background was then turned off, and ERGs were produced by the standard stimulus every 2 min for the first 30 min of dark adaptation. The a- and b-wave amplitudes were measured online (Neuropack m, QP-903B, Nihon Kohden, Tokyo, Japan). ERG was performed at day 7 after retinal ischemia.

2.6. Tissue processing

All *in vivo* experiments were performed using retinal and brain tissues. For retinal tissue preparation, mice were deeply anaesthetized with sodium pentobarbital (50 mg/kg, i.p.). Eye was quickly isolated, washed with saline and 4% paraformaldehyde (PFA). Eye was then nicked through pupil, post-fixed in 4% PFA for 24 h and finally transferred to 25% sucrose solution (in 0.1 M K^+-free PBS) overnight for cryoprotection. Following freeze in cryoembedding compound, retinal sections were prepared at 10 μm thickness for staining. For brain tissue preparation, mice were deeply anesthetized with sodium pentobarbital (50 mg/kg, i.p.) and perfused transcardially with 0.1 M K^+-free PBS, followed by 4% PFA. Brain was then quickly removed, post-fixed in 4% PFA and transferred immediately to 25% sucrose solution overnight. Brain was frozen in cryoembedding compound and coronal sections were cut at 30 μm thickness for staining.

2.7. Morphological assessment of retinal damages

For hematoxylin and eosin (H&E) staining, on the other hand, frozen retinal sections were washed with 0.1 M K^+-free PBS, immerged in Mayer's hematoxylin solution (WAKO, Osaka, Japan) for 5 min at room temperature (25 °C) and then washed with tap

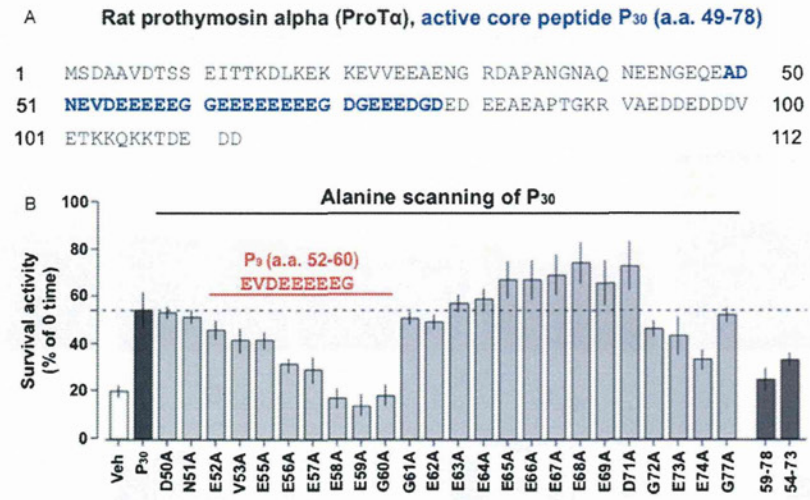

Fig. 1. Central 9-amino acid peptide in ProTα is an essential domain for its survival activity. (A) Amino acid (a.a.) sequence of rat ProTα and active core peptide P_{30}. Blue colored sequence indicates P_{30} (a.a 49–78). (B) Screening of essential amino acid residue of P_{30} in survival activity using alanine scanning of P_{30} and deletion mutant analysis. Survival activity of primary cultured cortical neurons was measured at 12 h after serum-free ischemic stress. Survival activity of P_{30} was significantly abolished by replacement of amino acids between E56 and G60 by alanine, whereas E52A, V53A, and E55A showed partial survival activity. However, the 54–73 amino acid peptide and the 59–78 amino acid peptide, C-terminus of P_{30}, have no significant survival activity. Red colored line and sequence indicate an essential 9-amino acid peptide P_9 and its survival activity. Dashed line indicates the level of the survival activity of P_{30}. (For interpretation of the references to color in this figure legend, the reader is referred to the web version of the article.)

water for 20 min. Following brief treatment with 95% ethanol, sections were immerged in eosin–alcohol solution (WAKO) for 4 min at 25 °C. Sections were dehydrated through a series of ethanol solutions, xylene, and over-slipped with Permount (Fisher Scientific, Waltham, MA, USA). Sections were then analyzed using a BZ-8000 microscope with BZ Image Measurement Software (KEYENCE, Osaka, Japan).

2.8. TTC staining

For 2,3,5-triphenyltetrazolium chloride (TTC) staining, brain was quickly removed at 24 h after cerebral ischemia (1 h tMCAO) followed by P_9 administration ($n = 6$ for each group), sectioned coronally with 1-mm thickness and washed with K^+-free PBS. Brain slices were incubated in 2% TTC (Sigma–Aldrich, St. Louis, MO, USA) in 0.9% NaCl in dark place for 15–20 min at room temperature (25 °C) and transferred in 4% PFA overnight. Images of brain slices were then collected by scanner, and infarct volume was calculated by Image J software (NIH, Bethesda, MD, USA).

2.9. Evaluation of damaged blood vessels

To perform fluorescence staining of blood vessels, biotinylated *Lycopersicon esculentum* (tomato) lectin (Vector Laboratories, Burlingame, CA, USA) was diluted with PBS and injected (1 mg/ml, 100 μl, i.v.) at 24 h after cerebral ischemia (1 h tMCAO). Mice were perfused 5 min after tomato lectin injection. Following tissue preparation as described in Section 2, coronal brain sections were washed with 0.1 M K^+-free PBS and blocked with 2% BSA in 0.1% PBST for 2 h at 25 °C. Sections were then incubated with Alexa Fluor 488 streptavidin conjugates (Molecular Probes, Eugene, OR, USA) for 2 h at room temperature (25 °C). Sections were thoroughly washed with PBS and cover-slipped with Perma Fluor. Images were collected using an LSM 710 confocal microscope with ZEN Software (Carl Zeiss, Oberkochen, Germany).

2.10. Behavioral assessments

Following P_9 administration with doses of 0.1, 0.3 and 1 mg/kg (i.v., $n = 7$, $n = 6$ and $n = 7$, respectively) 1 h after cerebral ischemia (1 h tMCAO), clinical scores were assessed at 24 h after the ischemic stress. Clinical score was evaluated in the following way: 0, no observable deficits; 1, failure to extend the forepaw fully; 2, circling; 3, falling to one side; 4, no spontaneous movement; 5, death. In this study, 0.5 point was added to each score when the motor dysfunction was severe for scores between 1 and 4.

2.11. Statistical analysis

All results are shown as means ± S.E.M. Two independent groups were compared using the Student's *t*-test. Multiple groups were compared using Dunnett's multiple comparison tests after a one-factor ANOVA or a Repeated Measures ANOVA. Survival rate was compared using Logrank test after Kaplan–Meyer method. $P < 0.05$ was considered significant.

3. Results

3.1. Identification of functionally active short 9-amino acid peptide

More recently, we succeeded in identifying 30-amino acid peptide (P_{30}: amino acids 49–78) from the sequence of ProTα, bearing neuroprotective activity *in vitro* and *in vivo* [17]. To design shorter amino acid peptide from P_{30} peptide in ProTα (Fig. 1A), we screened essential amino acid residue of P_{30} by use of alanine scanning technique (Fig. 1B). Following replacement of amino acids D50 and N51 by alanine (D50A and N51A), no change in survival activity of P_{30} in cultured cortical neurons against ischemic stress was observed at 12 h after the start of culture, whereas E52A, V53A, and E55A showed partial survival activity (Fig. 1B). Interestingly, the survival activity of P_{30} was markedly abolished by replacement of amino acids between E56 and G60 by alanine (Fig. 1B). On the other hand, the survival activity was absent in peptide comprised of 54–73 amino acid residues as well as in C-terminus of P_{30} (amino acids 59–78) against ischemic stress (Fig. 1B). These results indicated that 9-amino acid peptide (E52–G60) is core domain of P_{30} for its full neuroprotective action.